AD-A080 311 RENSSELAER POLYTECHNIC INST TROY NY DEPT OF MATHEMAT--ETC F/G 12/1
COLLOCATION WITH POLYNOMIAL AND TAUT SPLINES FOR SINGULARLY PER--ETC(U)
NOV 79 J E FLAHERTY, W MATHON AFOSR-75-2818

UNCLASSIFIED AFOSR-TR-80-0085 NL

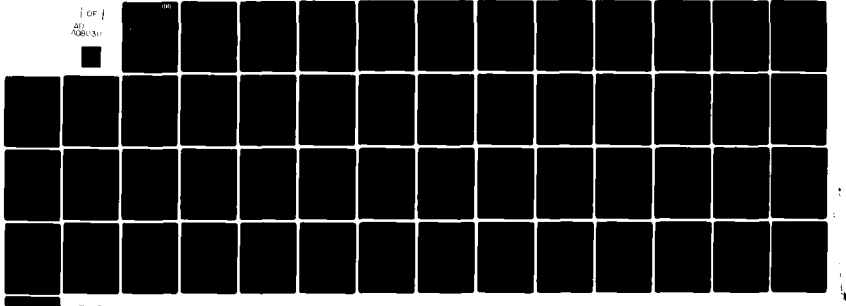

END
DATE FILMED
2-80
DDC

COLLOCATION WITH POLYNOMIAL AND TAUT SPLINES FOR SINGULARLY PERTURBED BOUNDARY VALUE PROBLEMS*

(10) Joseph E. Flaherty

and

William Mathon

Department of Mathematical Sciences
Rensselaer Polytechnic Institute
Troy, New York 12181

*This work was supported by the Air Force Office of Scientific Research, Grant Number AFOSR-75-2818.

80

ABSTRACT

Collocation methods using both cubic polynomials and splines in tension are developed for second order linear singularly-perturbed two-point boundary value problems. Rules are developed for selecting tension parameters and collocation points. The methods converge outside of boundary layer regions without the necessity of using a fine discretization. Numerical examples comparing the methods are presented.

1. Introduction

We consider the numerical solution by collocation methods of the singularly-perturbed second-order linear boundary value problem

$$Ly \equiv \varepsilon y'' + p(x)y' + q(x)y = f(x) \quad , \quad a \leq x \leq b \, , \tag{1.1}$$

$$\alpha_{11}y(a,\varepsilon) + \alpha_{12}y'(a,\varepsilon) = A, \quad \alpha_{21}y(b,\varepsilon) + \alpha_{22}y'(b,\varepsilon) = B \, , \tag{1.2}$$

where ε is a small positive parameter. The functions p,q, and f are assumed to be smooth functions of x on [a,b] which, along with α_{ij}, i, j = 1, 2, A, and B, may depend on ε provided they are bounded as $\varepsilon \to 0$. We further assume that (1.1,2) has a unique solution on [a,b] for all ε sufficiently small.

The problem (1.1,2) has been intensively studied analytically (cf. Cole [6], Eckhaus [11], or O'Malley [18]) and it is known that its solution generally has a multiscale character, i.e., it features regions called "boundary layers" where the solution varies rapidly. Away from the boundary layers, the solution is approximately determined by neglecting the $\varepsilon y''$ term in (1.1) and perhaps one or both of the boundary conditions (1.2).

The problem has also been extensively studied numerically, and it is known that most classical methods fail when ε is small relative to the mesh width h that is used for the discretization of the operator L. There are, however, several finite difference methods (cf. Abrahamson, Keller, and Kreiss [1], Berger, et al. [4], Il'in [16], Kreiss [17], and Pearson [19,20]), Galerkin-finite element methods (cf. Hemker [15], de Groen and Hemker [10], and Heinrich, et al. [13,14]), and methods based on singular perturbation theory (cf. Flaherty and O'Malley [12] and Steele [28]) that do not require h/ε to be small.

Our aim in this paper is to show that collocation methods with either piecewise polynomials or splines in tension can furnish accurate numerical approximations of (1.1,2) when either h/ε is small or large. Splines in tension were first used by Schweikert [26] as a means of eliminating spurious oscillations in curve fitting with cubic splines. They have been subsequently studied by Cline [5], Pruess [22], Späth [27], and de Boor [9, Chap. 16]. Between knot points a spline in tension, or a taut spline in the language of de Boor [9], is an L- spline satisfying the differential equation

$$(\tau'' - \rho^2\tau)'' = 0 , \tag{1.3}$$

subject to appropriate continuity conditions at the knots. The quantity ρ is called the tension parameter. When $\rho = 0$, τ is a cubic polynomial spline; however, when $\rho > 0$, the solution of (1.3) is a linear combination of the four functions 1, x, $e^{\rho x}$, $e^{-\rho x}$. The exponential functions should be better suited than polynomials at following the rapid variations that are typically found in singular perturbation problems. Indeed, exponentials have been used in the Galerkin methods of Hemker [15] and de Groen and Hemker [10], I1'in's difference method [16], and the singular perturbation methods of Flaherty and O'Malley [12] and Steele [28].

Equation (1.3) is the same as that for the transverse deflection of a classical Euler-Bernoulli elastic beam that is subjected to a tensile force proportional to ρ^2; hence, the name spline in tension.

In Section 2 of this paper, we construct a basis for the tnesion splines and use it to obtain the collocation equations. In Section 3, we obtain asymptotic approximations to the solution of (1.1,2) in the two special cases when $|p(x)| \geq \bar{p} > 0$ and when

$p(x) \equiv 0$ on $[a,b]$ and use these to select tension parameters. In Section 4, we discuss the selection of collocation points that are in some sense optimal and present some formal error estimates in regions not containing boundary layers. In Section 5, we apply our methods to some examples; and in Section 6, we discuss the results.

Not surprisingly, the results indicate that taut splines provide better approximations within boundary layers and polynomials provide better approximations elsewhere. This suggests the possibility of applying tension only within boundary layers. This would either require an a priori knowledge of the location of the boundary layers or an automatic procedure for finding them. A tentative procedure for automatically locating boundary layers is presented in Section 5.

We anticipate that our methods would be useful on other problems, such as initial-boundary value problems for parabolic partial differential equations involving diffusion, convection and/or reaction.

2. Collocation Equations and the Tension Spline Basis

In the usual method of collocation (cf. Ascher, Christiansen, and Russell [2], de Boor and Swartz [8], Russell [23], or Russell and Shampine [25]), one introduces a partition

$$\Delta_N \equiv \{a = x_0 < x_1 < \ldots < x_N = b\} \tag{2.1}$$

of $[a,b]$ into N subintervals and approximates the solution of (1.1,2) by piecewise polynomials $y_h(x) \in M(\Delta_N,k,m)$, where

$$M(\Delta_N,k,m) \equiv \{w \in C^m[a,b] \mid w_{\text{restr. to } I_i} \in P_k(I_i);\ i = 1,2,\ldots,N\} . \tag{2.2}$$

Here

$$I_i \equiv (x_{i-1},x_i) \tag{2.3}$$

and $P_k(E)$ denotes the class of polynomials having at most degree k on E. The dimension of $M(\Delta_n,k,m)$ is $N(k-m) + m + 1$ and one determines $y_h(x)$ by collocating at $N(k-m) + m - 1$ points $z_i \in [a,b]$, i.e., by enforcing

$$Ly_h(z_i) = f(z_i) , \quad i = 1,2,\ldots,N(k-m) + m - 1 , \tag{2.4}$$

and by requiring y_h to satisfy the boundary conditions (1.2). Convergence and the order of accuracy of these methods depend on m,k,Δ_N, and the choice of z_i and are discussed in, e.g., [8]. However, Ly_h should exist and necessary continuity conditions on $M(\Delta_N,k,m)$ are $k \geq 2$ and $m \geq 1$. In addition, de Boor and Swartz [8] show that the maximal order of convergence in the largest subinterval length is achieved by selecting the collocation points as an appropriate number of Gauss-Legendre points on each subinterval.

Unfortunately, collocation at the Gauss-Legendre points with piecewise polynomials is known to behave rather poorly on singularly-perturbed problems for any partition where ε is much smaller than the minimum subinterval length (cf. Hemker [15] and our Example 1 in Section 5). It would be overly restrictive and in most cases impractical to require a partition with subinterval lengths of order ε and we seek to avoid this situation by changing the locations of the collocation points and/or adding exponential functions to $M(\Delta_N,k,m)$. Thus, we also consider approximations $y_h(x) \in E(\Delta_N,k,m,\underset{\sim}{\rho})$, where

$$E(\Delta_N,k,m,\underset{\sim}{\rho}) \equiv \{w \in C^m[a,b] \mid w_{\text{restr. to } I_i} \in \text{span}\,(P_k(I_i), e^{\rho_i x/h_i}, e^{-\rho_i x/h_i}); \; i = 1,2,\ldots,N\} \tag{2.5}$$

and

$$h_i = x_i - x_{i-1}, \quad i = 1,2,\ldots,N. \tag{2.6}$$

The quantities ρ_i, $i = 1,2,\ldots,N$, are called tension parameters

and will subsequently be selected to approximate the rapidly varying part of the exact solution of (1.1,2).

In this paper, we have confined our attention to collocation with piecewise cubic polynomials belonging to $M(\Delta_N,3,1)$ and splines in tension or taut splines belonging to $E(\Delta_N,1,1,\underset{\sim}{\rho})$, which are both spaces of dimension 2(N+1). For reasons of computational convenience and efficiency, it is usual to construct a basis for $M(\Delta_N,3,1)$ that satisfies the $C^1[a,b]$ continuity requirement and where each element has support extending over only two subintervals. We proceed similarly for $E(\Delta_N,1,1,\underset{\sim}{\rho})$; thus, we write $y_h(x)$ in the form

$$y_h(x) = \sum_{i=0}^{N} [c_i\tau_i(x,\underset{\sim}{\rho}) + d_i\sigma_i(x,\underset{\sim}{\rho})] \tag{2.7}$$

where the basis $\tau_i(x,\underset{\sim}{\rho})$, $\sigma_i(x,\underset{\sim}{\rho})$, $i = 0,1,\ldots,N$, is defined in terms of the "canonical basis elements" η_0 and η_1 as follows:

$$\tau_i(x,\underset{\sim}{\rho}) = \begin{cases} \eta_0\left(\dfrac{x_i-x}{h_i},\ \rho_i\right), & x\in[x_{i-1},x_i] \\ \eta_0\left(\dfrac{x-x_i}{h_{i+1}},\ \rho_{i+1}\right), & x\in[x_i,x_{i+1}] \\ 0, & \text{otherwise} \end{cases} \tag{2.8}$$

and

$$\sigma_i(x,\underset{\sim}{\rho}) = \begin{cases} -h_i\eta_1\left(\dfrac{x_i-x}{h_i},\ \rho_i\right), & x\in[x_{i-1},x_i] \\ h_i\eta_1\left(\dfrac{x-x_i}{h_{i+1}},\ \rho_{i+1}\right), & x\in[x_i,x_{i+1}] \\ 0, & \text{otherwise} \end{cases} \tag{2.9}$$

The functions $\eta_0(s,\rho)$ and $\eta_1(s,\rho)$ are defined on $0 \le s \le 1$ as

$$(2.10)\quad \eta_0(s,\rho) = 1 - s + K_0\left[2s - 1 - \frac{\sinh \rho/2(2s-1)}{\sinh \rho/2}\right],$$

$$(2.11)\quad \eta_1(s,\rho) = \tfrac{1}{2}K_0\left[2s - 1 - \frac{\sinh \rho/2(2s-1)}{\sinh \rho/2}\right] + \tfrac{1}{2}K_1\left[1 - \frac{\cosh \rho/2(2s-1)}{\cosh \rho/2}\right],$$

where

$$(2.12)\quad K_0 = 1/\rho\omega(\rho/2),\quad K_1 = (1/\rho)\coth \rho/2,\quad \omega(z) = \coth z - 1/z .$$

Observe that η_0 and η_1 each satisfy the differential equation

$$(2.13)\qquad (\eta_k'' - \rho^2\eta_k)'' = 0 ,\quad 0 \le s \le 1 ,\quad k = 0,1,$$

subject to the boundary conditions

$$(2.14)\quad \eta_k(0,\rho) = \delta_{0k} ,\quad \eta_k(1,\rho) = 0 ,\quad \eta_k'(0,\rho) = \delta_{1k} ,\quad \eta_k'(1,\rho) = 0 ,\quad k = 0,1,$$

where δ_{ik} denotes the Kronecker delta and, in this context, $(\ )'$ denotes differentiation with respect to s. Using (2.14) and (2.7-9), we see that $c_i = y_h(x_i)$ and $d_i = dy_h(x_i)/dx$, $i = 0,1,\ldots,N$.

As ρ tends to zero η_0 and η_1 approach the usual canonical basis elements for $M(\Delta_N,3,1)$, i.e., that of a cubic Hermite interpolating polynomial on $0 \le s \le 1$. Thus,

$$(2.15)\quad \eta_0(s,\rho) = (1-s)^2(1+2s) + 0(\rho^2) ,\quad \eta_1(s,\rho) = s(1-s)^2 + 0(\rho^2) .$$

For large values of ρ η_0 and η_1 become

$$(2.16)\quad \eta_0(s,\rho) = 1 - s - \frac{1}{\rho-2}\left[2s-1+e^{-\rho s} - e^{-\rho(1-s)}\right] + 0(e^{-\rho}/\rho)$$

$$\eta_1(s,\rho) = \frac{\rho-1}{\rho(\rho-2)}\left[1-s-e^{-\rho s}\right] - \frac{1}{\rho(\rho-2)}\left[s-e^{-\rho(1-s)}\right] + 0(e^{-\rho}/\rho) .$$

Thus, in the interior of (0,1) η_0 and η_1 are asymptotically given by the linear functions

$$\eta_0(s,\rho) \sim (1-s) - (2s-1)/(\rho-2) ,\quad \eta_1(s,\rho) \sim (1-s)/\rho - (2s-1)/\rho(\rho-2) .$$

Both η_0 and η_1 converge uniformly on $0 \le s \le 1$ as $\rho \to \infty$ to 1-s and 0,

respectively; however, their derivatives exhibit boundary layer behavior at s = 0 and 1. Since τ_i and σ_i (via. (2.8,9)) behave similarly at the knots x_{i-1}, x_i, x_{i+1}, the numerical approximation y_h may have internal boundary layer jumps of height $0(1/\rho)$ even when the exact solution is smooth. We demonstrate this phenomena in example 1 of Section 5. The functions η_0 and η_1 are plotted for a small and a large values of ρ in Figures 1a and 1b, respectively.

A discrete system for determining c_i, d_i, $i = 0,1,\ldots,N$ is obtained for a given set of tension parameters $\rho_i, i=1,2,\ldots,N$ by collocating at 2N points $z_i, i=1,2,\ldots,N$ on [a,b] and by satisfying the boundary conditions (1.2). For simplicity we place two collocation points symmetrically disposed on each subinterval, i.e.,

$$z_{2i-1} = x_{i-1} + t_i h_i \ , \quad z_{2i} = x_{i-1} + (1-t_i)h_i \ , \quad i = 1,2,\ldots,N, \tag{2.17}$$

for an appropriate choice of $t_i \in [0,1/2)$. Then, using (2.17), (2.7-9), and (1.1) in (2.4) we find the discrete system on I_i to be

$$\begin{bmatrix} \ell_{i1}(t_i) & \ell_{i2}(t_i) & \ell_{i3}(t_i) & \ell_{i4}(t_i) \\ \ell_{i1}(1-t_i) & \ell_{i2}(1-t_i) & \ell_{i3}(1-t_i) & \ell_{i4}(1-t_i) \end{bmatrix} \begin{bmatrix} c_{i-1} \\ d_{i-1} \\ c_i \\ d_i \end{bmatrix} = \begin{bmatrix} \hat{f}_i(t_i) \\ \hat{f}_i(1-t_i) \end{bmatrix}, \tag{2.18}$$

$$i = 1,2,\ldots,N$$

where

$$\begin{aligned} \ell_{i1}(t) &= (\varepsilon/h_i^2)\eta_0''(t,\rho_i) + (\hat{p}_i(t)/h_i)\eta_0'(t,\rho_i) + \hat{q}_i(t)\eta_0(t,\rho_i) \ , \\ \ell_{i2}(t) &= (\varepsilon/h_i)\eta_1''(t,\rho_i) + \hat{p}_i(t)\eta_1'(t,\rho_i) + \hat{q}_i(t)h_i\eta_1(t,\rho_i) \ , \\ \ell_{i3}(t) &= (\varepsilon/h_i^2)\eta_0''(1-t,\rho_i) - (\hat{p}_i(t)/h_i)\eta_0'(1-t,\rho_i) + \hat{q}_i(t)\eta_0(1-t,\rho_i) \ , \\ \ell_{i4}(t) &= -[(\varepsilon/h_i)\eta_1''(1-t,\rho_i) - \hat{p}_i(t)\eta_1'(1-t,\rho_i) + \hat{q}_i(t)\eta_1(1-t,\rho_i)] \ , \end{aligned} \tag{2.19}$$

and $\hat{f}_i(t) \equiv f(x_{i-1}+th)$, etc. Substituting (2.7-9) into (1.2) gives the boundary conditions

$$\alpha_{11}c_0 + \alpha_{12}d_0 = A\ , \quad \alpha_{21}c_N + \alpha_{22}d_N = B\ . \tag{2.20}$$

Thus, the 2(N+1) dimensional discrete system (2.18-20) has the following structural form

$$\begin{bmatrix} x & x & & & & & & & & \\ x & x & x & x & & & & & & \\ x & x & x & x & & & & & & \\ & & x & x & x & x & & & & \\ & & x & x & x & x & & & & \\ & & & \cdot & \cdot & \cdot & & & & \\ & & & & & x & x & x & x & \\ & & & & & x & x & x & x & \\ & & & & & & & x & x & \end{bmatrix} \begin{bmatrix} c_0 \\ d_0 \\ c_1 \\ d_1 \\ \cdot \\ \cdot \\ \cdot \\ c_N \\ d_N \end{bmatrix} = \begin{bmatrix} A \\ \hat{f}_1(t_1) \\ \hat{f}_1(1-t_1) \\ \cdot \\ \cdot \\ \cdot \\ \hat{f}_N(t_N) \\ \hat{f}_N(1-t_N) \\ B \end{bmatrix}, \tag{2.21}$$

where each x denotes a nonzero entry. We solve (2.18-20) for prescribed values of ρ_i and t_i, i = 1,2,...,N, by an alternating row and column pivoting algorithm due to Varah [29]. This procedure is numerically stable and requires no storage additional to that needed for the nonzero entries in (2.21).

3. Asymptotic Solutions, Green's Functions, and the Selection of Tension Parameters

In this section, we present asymptotic approximations of the solution of (1.1,2) and of its Green's function. They will be used to select the tension parameters and in Section 4 to select collocation points. We shall not attempt to do this in all generality, but rather by considering two special cases of the problem

(3.1) $$Ly \equiv \varepsilon y'' + p(x)y' + q(x)y = f(x) \quad , \quad a \le x \le b \ ,$$

(3.2) $$y(a,\varepsilon) = A \ , \quad y(b,\varepsilon) = B \ ,$$

when (Problem 1) $|p(x)| \ge \bar{p} > 0$ and (Problem 2) when $p(x) \equiv 0$, $q(x) \le \bar{q} < 0$ for $x \in [a,b]$. In either case, any boundary layers are at the ends of $[a,b]$; thus, there are no turning points and no interior nonuniformities. We consider such problems among the examples of Section 5.

The Green's function $G(x,\xi)$ associated with the operator L and homogeneous boundary conditions (3.2) on the interval $[a,b]$ satisfies

(3.3) $$L^*G(x,\xi) \equiv \varepsilon G_{\xi\xi} - (p(\xi)G)_\xi + q(\xi)G = 0, (a,x) \cup (x,b),$$

(3.4a) $$G(x,a) = G(x,b) = 0 \ ,$$

(3.4b) $$G(x,x^+) - G(x,x^-) = 0 \ ,$$

(3.4c) $$G_\xi(x,x^+) - G_\xi(x,x^-) = 1/\varepsilon \ ,$$

where the subscript ξ denotes partial differentiation.

We use the WKB method to construct our asymptotic approximations of the solutions of (3.1,2) and (3.3,4). Since the details of this method are well known (cf. Wassow [30]), we only present the results and omit their development.

3.1. Problem 1: $|p(x)| \ge \bar{p} > 0$ for $x \in [a,b]$

We consider the case when $p(x) > 0$ on $[a,b]$. The case when $p(x) < 0$ is handled in an analogous manner. Using the WKB method, we find the following $0(\varepsilon)$ approximations to the two fundamental solutions of (3.1) (cf. Hemker [15]):

3.5a,b) $$Y(x,\xi) = \exp\{\int_x^\xi q(z)/p(z)dz\} \ , \quad \Pi(\xi,x) = \exp\{-\int_\xi^x (p(z)/\varepsilon - q(z)/p(z))dz \ .$$

The solution of (3.1) satisfying the boundary conditions (3.2) is given by

(3.6a) $$y(x,\varepsilon) = Y_R(x) + [A - Y_R(a)]\Pi(a,x) + 0(\varepsilon)$$

where

(3.6b) $$Y_R(x) = BY(x,b) - \int_x^b (f(z)/p(z))Y(x,z)dz \ .$$

The term $[A - Y_R(a)]\Pi(a,x)$ is exponentially small outside of a boundary layer of width $0(\varepsilon)$ near $x = a$. For $a < x \leq b$ $y(x,\varepsilon) \sim Y_R(x)$, where $Y_R(x)$ is the solution of the reduced problem

(3.7a) $$p(x)Y_R'(x) + q(x)Y_R(x) = f(x) \quad , \quad a \leq x \leq b \quad ,$$

(3.7b) $$Y_R(b) = B \quad ,$$

obtained by neglecting the $\varepsilon y''$ term in (3.1) and the boundary condition (3.2) at $x = a$. The problem with $p(x) < 0$ has a solution with a boundary layer near $x = b$ and a reduced solution satisfying (3.7a) subject to the initial condition $Y_R(a) = A$.

In a similar manner, an $0(\varepsilon)$ approximation to $G(x,\xi)$ satisfying (3.3,4) is found as

(3.8a) $$G(x,\xi) = \alpha(x)\{\Pi(\xi,b)Y^*(a,b)[\Pi(a,x) - Y^*(x,a)] - \Pi(a,x)Y^*(a,\xi) + \begin{cases} \Pi(\xi,x) & , \ a \leq \xi \leq x \\ Y^*(x,\xi) & , \ x \leq \xi \leq b \end{cases}\} + 0(\varepsilon)$$

where

(3.8b) $$\alpha(x) = -p(x)/[p^2(x) - 2\varepsilon q(x) + \varepsilon p'(x)] \ ,$$

(3.8c) $$Y^*(x,\xi) = \exp\{\int_x^\xi (q(z) - p'(z))/p(z)dz \quad ,$$

and $\Pi(\xi,x)$ is as in (3.5b). As a function of ξ, $G(x,\xi)$ has boundary layers at $\xi = b^-$ and $\xi = x^-$.

3.2. Problem 2: $p(x) \equiv 0$, $q(x) \leq \bar{q} < 0$ for $x\varepsilon[a,b]$.

In this case, the WKB method gives the following $0(\sqrt{\varepsilon})$ approximations to the two fundamental solutions of (3.1) (cf. Hemker [15]).

(3.9a,b) $$\Pi_1(x,\xi) = q(x)^{-1/4}\Pi(x,\xi) \quad , \quad \Pi_2(x,\xi) = q(x)^{-1/4}\Pi(\xi,x)$$

where for this problem

$$\Pi(\xi,x) = \exp\left\{-\int_{\xi}^{x} \sqrt{-q(z)/\varepsilon}\, dz\right\} . \tag{3.9c}$$

The character of the solution depends critically on the sign of $q(x)$. When $q(x) < 0$, the solution is exponential; and when $q(x) > 0$, the solution oscillates rapidly with period $2\pi\sqrt{\varepsilon/q(x)}$. We would not expect taut spline approximations to be useful in the oscillatory case and, thus, we confine our attention to problems with $q(x) < 0$ on $[a,b]$. The use of "splines under compression" for oscillatory problems is currently under investigation by Coyle and Flaherty [7].

Using (3.9), the solution of (3.1,2) is given as

$$\begin{aligned} y(x,\varepsilon) = {} & [A - f(a)/q(a)][q(a)/q(x)]^{1/4}\Pi(a,x) \\ & + [B - f(b)/q(b)][q(b)/q(x)]^{1/4}\Pi(x,b) + f(x)/q(x) + 0(\sqrt{\varepsilon}) . \end{aligned} \tag{3.10}$$

Outside of the boundary layers, which extend over $0(\sqrt{\varepsilon})$ neighborhoods of $x = a$ and b, the solution $y(x,\varepsilon) \sim Y_R(x)$, where $Y_R(x)$ is the solution of the reduced problem

$$q(x)Y_R(x) = f(x) ,$$

obtained by neglecting the $\varepsilon y''$ term in (3.1) and both boundary conditions (3.2).

Problem 2 is self-adjoint, so the WKB approximations (3.9) can also be used to construct the following $0(1)$ approximation to $G(x,\xi)$ satisfying (3.3,4):

$$\begin{aligned} G(x,\xi) = {} & \tfrac{1}{2}[\varepsilon^2 q(x)q(\xi)]^{-1/4}\{\Pi(a,x)\Pi(a,\xi) + \Pi(x,b)\Pi(\xi,b) \\ & - \begin{cases} \Pi(\xi,x) , & a \le \xi \le x \\ \Pi(x,\xi) , & x \le \xi \le b \end{cases} + 0(\sqrt{\varepsilon})\} . \end{aligned} \tag{3.11}$$

As a function of ξ, $G(x,\xi)$ has boundary layers on both sides of $\xi = x$, and is unbounded as $0(1/\sqrt{\varepsilon})$ as $\varepsilon \to 0$.

3.3. Selection of Tension Parameters

We want the tension parameters to approximate the rapidly decaying solutions (3.5b) or (3.9) of Problems 1 or 2, respectively, and so we choose ρ_i on the subinterval I_i as

$$\rho_i = h_i \begin{cases} |p(x_k)/\varepsilon - q(x_k)/p(x_k)| \ , & \text{if } |p(x_{i-1})+p(x_i)|/\varepsilon \geq |q(x_{i-1})+q(x_i)| \\ \sqrt{-[q(x_{i-1})+q(x_i)]/2\varepsilon} \ , & \text{if } |p(x_{i-1})+p(x_i)|/\varepsilon < |q(x_{i-1})+q(x_i)| \end{cases} , \tag{3.12a}$$

$$i = 1,2,\ldots,N,$$

where

$$k = \begin{cases} i-1 \ , & \text{if } [p(x_{i-1}) + p(x_i)]/\varepsilon > 0 \\ i \ , & \text{if } [p(x_{i-1}) + p(x_i)]/\varepsilon < 0 \end{cases} . \tag{3.12b}$$

Thus, for Problem 1 with $p(x) > 0$ on $[a,b]$

$$\rho_i = h_i |p(x_{i-1})/\varepsilon - q(x_{i-1})/p(x_{i-1})| \ , \tag{3.13a}$$

and for Problem 2

$$\rho_i = h_i \sqrt{-[q(x_{i-1}) + q(x_i)]/2\varepsilon} \ . \tag{3.13b}$$

However, we use (3.12) computationally even when the conditions of Problem 1 or 2 are not satisfied, e.g., when there are turning points.

The solution of the collocation equations (2.18-20) with the tension parameters specified by (3.12) will give the exact solution of (1.1,2), for any choice of $t_i \in [0,1/2)$, whenever $f(x)$ is a linear polynomial and either 1) $p(x) \equiv \bar{p}$ and $q(x) \equiv 0$ or 2) $p(x) \equiv 0$ and $q(x) \equiv \bar{q} < 0$. This is because the solutions of these problems are elements of the approximating space $E(\Delta_N,1,1,\underset{\sim}{\rho})$.

We close this section by applying the method of collocation with splines under tension to the example

(3.14) $Ly \equiv \varepsilon y'' + p(x)y' = f(x)$, $a \le x \le b$, $y(a) = A$, $y(b) = B$,

with $p(x) > 0$ on $[a,b]$. Using (3.5,6) the solution of this problem is

(3.15a) $$y(x,\varepsilon) = Y_R(x) + [A - Y_R(a)] \exp\left\{-\int_a^x (p(z)/\varepsilon)dz\right\}$$

where

(3.15b) $$Y_R(x) = B - \int_x^b (f(z)/p(z))dz \ .$$

For the present, we choose $t_i = 0$ and then use (2.10-12) and (2.19) in (2.18) to obtain the discrete system

$$(\varepsilon\rho_i/h_i)\left[\left(\frac{\nabla c_i}{h_i} - \frac{1}{2}\mu d_i\right)\omega^{-1}(\rho_i/2) + \frac{1}{2}\nabla d_i \coth \rho_i/2\right] + p(x_{i-1})d_{i-1} = f(x_{i-1}),$$

(3.16) $$(\varepsilon\rho_i/h_i)\left[\left(\frac{\nabla c_i}{h_i} - \frac{1}{2}\mu d_i\right)\omega^{-1}(\rho_i/2) - \frac{1}{2}\nabla d_i \coth \rho_i/2\right] + p(x_i)d_i = f(x_i),$$

$$i = 1,2,\ldots,N$$

$$c_0 = A \ , \quad c_N = B$$

where

(3.17) $$\nabla(\ )_i \equiv (\ )_i - (\ )_{i-1} \ , \quad \mu(\ )_i \equiv (\ )_i + (\ )_{i-1} \ ,$$

and $\omega(z)$ is defined by (2.12). Using (3.13a) we select $\rho_i = h_i p(x_{i-1})/\varepsilon$ and assume that the partition has been chosen so that $\rho_i >> 1$, $i = 1,2,\ldots,N$. In fact, suppose that ρ_i is large enough to approximate $\omega(\rho_i/2)$ and $\coth \rho_i/2$ by $(1-2/\rho_i)$ and 1, respectively. Then (3.16) become

(3.18)
$$(\varepsilon/h_i)(2\nabla c_i/h_i - \mu d_i) + p(x_{i-1})\nabla c_i/h_i = f(x_{i-1}) \ ,$$
$$(\mu p(x_i))d_i = \mu f(x_i) \ , \quad i = 1,2,\ldots,N, \quad c_0 = A, \quad c_N = B$$

Thus, the solution is approxiamtely determined as the solution of

(3.19a,b) $$c_N = B \ , \quad p(x_{i-1})\nabla c_i/h_i = f(x_{i-1}) + 0(\varepsilon/h_i) \ , \ i = N, N-1,\ldots,2,$$

(3.19c) $$(\mu p(x_i))d_i = \mu f(x_i) \ , \quad i = N,N-1,\ldots,1,$$

(3.19d,e) $c_0 = A$, $d_0 = -(p(a)/\varepsilon)[c_0 - c_1 + h_1 f(a)/p(a) + 0(\varepsilon/h_1)]$.

Equations (3.19a,b,c) can be recognized as $0(h)$ (where h is the maximum subinterval length) "upwind" difference approximations to the reduced problem, while (3.19e) gives the initial slope of the solution in the boundary layer correct to $0(h/\varepsilon)$.

4. Selection of Collocation Points

Our aim in this section is to suggest some special choices of collocation points that may be used to reduce the errors in methods for Problems 1 and 2. We confine our attention to the two limiting cases of zero tension ($\rho_i \equiv 0$) and large tension ($\rho_i >> 1$) for $i = 1,2,\ldots,N$. For simplicity, we consider uniform partitions with $h = h_i$, $i = 1,2,\ldots,N$, and assume that $hp(x)/\varepsilon >> 1$ for Problem 1 and $h\sqrt{-q(x)/\varepsilon} >> 1$ for Problem 2. No detailed rigorous error analysis will be given; however, some formal error estimates are obtained on subintervals not containing boundary layers.

4.1. Error Formulas

It is well known (cf. [8], [23], or [24]) that the pointwise error in collocation methods for (1.1,2) satisfies an equation of the form

$$(4.1) \qquad e^{(k)}(x) \equiv y^{(k)}(x) - y_h^{(k)}(x) = \int_a^b \frac{\partial^k}{\partial x^k} G(x,\xi) r(\xi) d\xi \ , \quad k = 0,1$$

where the residual

$$(4.2) \qquad r(\xi) = Ly(\xi) - Ly_h(\xi) = f(\xi) - Ly_h(\xi) \ .$$

It is convenient to introduce the local transformation

$$(4.3) \qquad \xi = x_{i-1} + hs \ , \quad 0 \le s \le 1$$

on the subinterval I_i and, as in Section 2, let $\hat{f}_i(s) \equiv f(x_{i-1}+hs)$, etc. Then (4.1) becomes

$$(4.4a)\qquad e^{(k)}(x) = h\sum_{i=1}^{N}\int_0^1 \frac{\partial^k}{\partial x^k} G(x, x_{i-1}+hs)\,\hat{r}_i(s)\,ds, \quad k = 0,1,$$

where

$$(4.4b)\qquad \hat{r}_i(s) = \hat{f}_i(s) - \hat{L}_i\hat{y}_{h_i}(s) ,$$

$$(4.5a)\qquad \hat{L}_i\hat{y}_i(s) = (\varepsilon/h^2)\hat{y}_i''(s) + \hat{L}_{R_i}\hat{y}_i(s) ,$$

and $\hat{L}_{R_i}$ is the reduced operator

$$(4.5b)\qquad \hat{L}_{R_i}\hat{y}_i(s) = (\hat{p}_i(s)/h)\hat{y}_i'(s) + \hat{q}_i(s)\hat{y}_i(s) .$$

Let $P\hat{f}_i(s)$ be the linear interpolant

$$(4.6)\qquad P\hat{f}_i(s) = [(1-t_i-s)\hat{f}_i(t_i) + (s-t_i)\hat{f}_i(1-t_i)]/(1-2t_i)$$

to $\hat{f}_i(s)$ at the two collocation points $s = t_i$ and $1 - t_i$ on I_i. Since the collocation equations (2.4,17) imply $\hat{L}_i\hat{y}_{h_i} = \hat{f}_i$ at $s = t_i$, $1 - t_i$, we have $P\hat{L}_i\hat{y}_{h_i} = P\hat{f}_i$ and (4.4a) may be written as

$$(4.7)\qquad e^{(k)}(x) = h\sum_{i=1}^{N}\int_0^1 \frac{\partial^k}{\partial x^k} G(x, x_{i-1}+hs)(1-P)\hat{r}_i(s)\,ds , \quad k = 0,1 .$$

The interpolation error

$$(4.8)\qquad (1-P)\hat{r}_i(s) = (s-t_i)(s-1-t_i)\hat{r}_i[t_i, 1-t_i, s] ,$$

where $\hat{r}_i[s_0, s_1, \ldots, s_k]$ denotes the k th divided difference of $\hat{r}_i$ at the points $s_0, s_1, \ldots, s_k$. This form of $(1-P)\hat{r}_i(s)$ suffices when $\rho_i \equiv 0$; however, when $\rho_i >> 1$ a more detailed form is needed. In this case, we assume that ρ_i is large enough to neglect terms of $0(e^{-\rho_i/2})$ relative to unity and use the large tension approximations (2.16) and (2.7-9) in (4.5) to get

$$(4.9)\qquad \hat{L}_i\hat{y}_{h_i} = \frac{\rho_i}{\rho_i-2}\left[e^{-\rho_i s}\beta_i\hat{u}_i(s) - e^{-\rho_i(1-s)}\gamma_i\hat{v}_i(s)\right] + \hat{L}_{R_i}\hat{y}_{h_i}(s) ,$$

where

$$(4.10)\qquad \beta_i = \nabla c_i/h - d_{i-1} - (\nabla d_i)/\rho_i , \quad \gamma_i = \nabla c_i/h - d_i + (\nabla d_i)/\rho_i$$

(4.11) $\hat{u}_i(s) = \varepsilon\rho_i/h - \hat{p}_i(s) + \hat{q}_i(s)h/\rho_i$, $\hat{v}_i(s) = \varepsilon\rho_i/h + \hat{p}_i(s) + \hat{q}_i(s)h/\rho_i$,

and $\hat{Y}_{h_i}(s)$ is the linear polynomial part of $\hat{y}_{h_i}(s)$; thus,

(4.12) $$\hat{L}_{R_i}\hat{Y}_{h_i}(s) = \frac{\rho_i}{\rho_i-2}\,[\hat{p}_i(s)(\nabla c_i/h - \mu d_i/\rho_i)$$

$$+ \hat{q}_i(s)[(c_{i-1} + d_{i-1}h/\rho_i)(1-s-1/\rho_i) + (c_i - d_ih/\rho_i)(s-1/\rho_i)] .$$

The choice of ρ_i given by (3.12) makes $\hat{u}_i(s) = 0(h)$ when $\hat{p}_i(s) > 0$ on I_i, $\hat{v}_i(s) = 0(h)$ when $\hat{p}_i(s) < 0$ on I_i, and $\hat{u}_i(s) = \hat{v}_i(s) = 0(h^2/\rho_i)$ when $\hat{p}_i(s) \equiv 0$ on I_i .

Using (4.9) and (4.4b), we have

(4.13) $$(1-P)\hat{r}_i(s) = (s-t_i)(s-1+t_i)\{\hat{f}_i[t_i,1-t_i,s] - \hat{L}_{R_i}\hat{Y}_{h_i}[t_i,1-t_i,s]\}$$

$$- \frac{\rho_i}{\rho_i-2}\{\beta_i\hat{u}_i(s)g(s,t_i) - \gamma_i\hat{v}_i(s)g(1-s,t_i)$$

$$+ (s-t_i)(s-1+t_i)\,\frac{e^{-\rho_i t_i} - e^{-\rho_i(1-t_i)}}{1-2t_i}\,(\beta_i\hat{u}_i[1-t_i,s]+\gamma_i\hat{v}_i[1-t_i,s])$$

$$-(s-t_i)(s-1+t_i)\Big(e^{-\rho_i t_i}\beta_i\hat{u}_i[t_i,1-t_i,s]+e^{-\rho_i(1-t_i)}\gamma_i\hat{v}_i[t_i,1-t_i,s]\Big)\Big\},$$

where

(4.14) $$g(s,t_i) = [(1-2t_i)e^{-\rho_i s} + (s-1+t_i)e^{-\rho_i t_i} - (s-t_i)e^{-\rho_i(1-t_i)}]/(1-2t_i) .$$

The assumption that terms of $0(e^{-\rho_i/2})$ are negligible will specifically allow us to drop all terms in (4.13,14) involving the factor $e^{-\rho_i(1-t_i)}$ since $t_i < 1/2$. This will be done in all further uses of (4.13,14) except where noted.

It remains to use the formulas (4.8) or (4.13) for $(1-P)\hat{r}_i(s)$ together with the approximations (3.8) or (3.11) for the Green's functions in (4.7) and find appropriate choices for collocation points. One problem is that the errors given by (4.7) depend on the unknown numerical solution y_h. This would not be a serious

difficulty if y_h and y_h' were bounded as $\varepsilon \to 0$ for fixed h. We have shown by example in Section 3 that c_i and d_i (hence, y_h and y_h') are bounded away from the boundary layer region for $\varepsilon/h << 1$ when $t_i = 0$ and ρ_i is selected according to (3.12). It is reasonable to assume that this remains so when t_i is sufficiently small; however, it is also relatively easy to show that d_i can be unbounded at every knot point as $\varepsilon/h \to 0$ when $\rho_i = 0$ and t_i are the Gauss-Legendre points. Little is known about the behavior of the numerical solution for other choices of t_i and ρ_i. In this paper, we shall not attempt to find conditions for y_h to be bounded as $\varepsilon \to 0$, but rather we shall make some suggestions for collocation points that should generally reduce the error in methods for Problems 1 and 2. We note in passing that if y_h and y_h' were bounded, arguments similar to those used by Pruess [21] or Russell and Christiansen [24] on related non singularly-perturbed problems could be used to remove the dependence on y_h from the leading order terms in e(x).

4.2. Collocation Points for Problem 1

We again consider the case when $p(x) \geq \bar{p} > 0$ for $x \in [a,b]$. Let x be a knot point, say x_j, so that there are no discontinuities in derivatives of the Green's function on any subinterval and apply the transformation (4.3) to (3.5b) and (3.8c) to get

$$\Pi(x_{i-1} + hs, x_j) = \Pi(x_i, x_j)\hat{\pi}_i(s) = \delta_{ij}\hat{\pi}_i(s) , \quad i \leq j \tag{4.15a}$$

$$Y^*(x_j, x_{i-1} + hs) = Y^*(x_j, x_{i-1})\hat{\zeta}_i(s) , \quad i > j \tag{4.15b}$$

where

$$\hat{\pi}_i(s) = \exp\{-h\int_s^1 [\hat{p}_i(z)/\varepsilon - \hat{q}_i(z)/\hat{p}_i(z)]dz , \tag{4.15c}$$

$$\hat{\zeta}_i(s) = \exp\{h\int_0^s [(\hat{q}_i(z) - \hat{p}_i'(z))/\hat{p}_i(z)]dz . \tag{4.15d}$$

The last form of (4.15a) follows from our assumption that terms of $0(e^{-\rho_i/2})$ are negligible, hence, the boundary layer in $\Pi(x_i,x_j)$ at x_j is well within subinterval I_j.

Using (3.8a) and (4.15) in (4.7) we have

$$e(x_j) = h[\tilde{Y}^*(a,b)\delta_{j0} - \tilde{Y}^*(x_j,b)]S_N - h\delta_{j0}\sum_{i=1}^{N}\tilde{Y}^*(a,x_{i-1})R_i$$

$$+ h\alpha(x_j)S_j + h\sum_{i=j+1}^{N}\tilde{Y}^*(x_j,x_{i-1})R_i \ , \tag{4.16a}$$

$$e'(x_j) = -h\{\tilde{Y}^*(a,b)[\rho_j^*/h - \alpha'(x_j)/\alpha(x_j)]\delta_{j0} + \tilde{Y}_x^*(x_j,b)\ S_N$$

$$+ h\ [\rho_j^*/h - \alpha'(x_j)/\alpha(x_j)]\delta_{j0}\sum_{i=1}^{N}\tilde{Y}^*(a,x_{i-1})R_i$$

$$- h\alpha(x_j)[\rho_j^*/h - \alpha'(x_j)/\alpha(x_j)]S_j + h\sum_{i=j+1}^{N}\tilde{Y}_x^*(x_j,x_{i-1})R_i \tag{4.16b}$$

where

$$\rho_j^* \equiv h[p(x_j)/\varepsilon - q(x_j)/p(x_j)], \quad \tilde{Y}^*(x_j,x_i) \equiv \alpha(x_j)Y^*(x_j,x_i) \ , \tag{4.17,18}$$

and

$$S_i = \int_0^1 \hat{\pi}_i(s)(1-P)\hat{r}_i(s)ds \ , \quad R_i = \int_0^1 \hat{\zeta}_i(s)(1-P)\hat{r}_i(s)ds \ . \tag{4.19a,b}$$

We call ρ_j^* the adjoint tension parameter and note that $\rho_j^* = \rho_{j+1}$ when the tension parameters are selected according to (3.13a). Observe that ρ_j^* is large whenever $hp(x)/\varepsilon$ is large and this can induce large errors in $e'(x_j)$ (cf. (4.16b)). These large errors can be confined to the boundary layer near $x = a$ if S_j is sufficiently small. *However, in order for* $e'(x_j)$ *to be small within the boundary layer* R_i, $i = 1,2,\ldots,N$, must also be sufficiently small. In this paper, we have concentrated on producing good approximations outside of boundary layer subintervals.

We first consider the taut spline approximation where $(1-P)\hat{r}_i(s)$ is given by (4.13,14). Expanding $f(x)$, $p(x)$, and $q(x)$ in Taylor's

series about a suitable point on I_i would reveal that $\hat{f}_i[t_i,1-t_i,s]$ and $\hat{u}_i[t_i,1-t_i,s]$ are $0(h^2)$ while $\hat{u}_i[1-t_i,s]$ and $\hat{v}_i[1-t_i,s]$ are $0(h)$. As previously noted, the choice of ρ_i given by (3.13a) makes $\hat{u}_i(s)$ of $0(h)$ and

$$\hat{v}_i(s) = \hat{p}_i(0) + \hat{p}_i(s) + 0(h/\rho_i) \quad . \tag{4.20}$$

If we further assume that c_i, d_i/ρ_i, and $\nabla c_i/h$ are bounded then $\hat{L}_{R_i}\hat{Y}_{h_i}[t_i,1-t_i,s]$ is $0(h^2)$, and to leading order (4.13,14) become

$$(1-P)\hat{r}_i(s) \simeq \gamma_i \hat{v}_i(s) g(1-s,t_i) \quad . \tag{4.21}$$

This is not surprising since this term is due to the presence of the $e^{-\rho_i(1-s)}$ functions in the taut spline approximation and these functions are not present in the exact solution of Problem 1.

Substituting (4.21) into (4.19) gives

$$S_i \simeq \gamma_i \int_0^1 \hat{\pi}_i(s) g(1-s,t_i) \hat{v}_i(s) ds \quad , \quad R_i \simeq \gamma_i \int_0^1 \hat{\zeta}_i(s) g(1-s,t_i) \hat{v}_i(s) ds \quad . \tag{4.22a,b}$$

S_i may be further approximated by using Laplace's method (cf. Bender and Orszag [3, Chap. 6]). The essential idea is that $\hat{\pi}_i(s)$ is exponentially small outside of a small neighborhood of $s = 1$ when $\hat{hp}_i(s)/\varepsilon$ is large; hence, the integrand in (4.15c) may be replaced by its value at $s = 1$. Using (4.17) this gives

$$S_i \simeq \gamma_i \int_0^1 e^{-\rho_i^*(1-s)} g(1-s,t_i) \hat{v}_i(s) ds. \tag{4.23}$$

Now, we see that S_i may be reduced in magnitude by selecting t_i such that $e^{-\rho_i^*(1-s)}$ is orthogonal to $g(1-s,t_i)$, i.e., using (4.14) we require

$$\int_0^1 e^{-\rho_i^*(1-s)} g(1-s,t_i) ds = \frac{1}{\rho_i^*} \left[\frac{1}{1+\rho_i/\rho_i^*} - \frac{1-t_i-1/\rho_i^*}{1-2t_i} e^{-\rho_i t_i}\right] = 0 \quad . \tag{4.24}$$

If terms of $0(1/\rho_i^*)$ are neglected, this implies

$$t_i = (1/\rho_i) \ln (1+\rho_i/\rho_i^*) \quad , \quad i = 1,2,\ldots,N \quad . \tag{4.25}$$

We refer to this choice of t_i as Method 1. It can only be used when ρ_i and ρ_i^* are such that $t_i < 1/2$. When ρ_i and ρ_i^* are large $t_i = 0(1/\rho_i)$ and collocation is performed near the ends of each subinterval. Using (4.14), (4.20), and (4.25) in (4.22b) implies

$$R_i \simeq \gamma_i \hat{\zeta}_i(1)\hat{v}_i(1)e^{-\rho_i t_i} \simeq \gamma_i \hat{p}_i(1)\hat{\zeta}_i(1) \quad . \tag{4.26}$$

If both c_i and d_i were bounded outside of the boundary layer, then γ_i would be $0(h)$ (cf. (4.10)). Thus, from (4.16) the best that we could expect from Method 1 is for $e(x_j)$ and $e'(x_j)$ to be $0(h)$. The computational evidence in Section 5 indicates that this is the case.

A second possibility is to select t_i so that R_i given by (4.22b) is reduced in magnitude. This can be done by requiring

$$\int_0^1 g(1-s,t_i)ds = 0.$$

Using (4.14) this leads to

$$t_i = \frac{1}{2}\left[1 - \frac{2}{\rho_i}\cosh^{-1}\left(\frac{2}{\rho_i}\sinh\frac{\rho_i}{2}\right)\right] , \tag{4.27}$$

and we refer to this choice of t_i as Method 2. We retained the $0(e^{-\rho_i(1-t_i)})$ term in (4.14) when obtaining (4.27) in order that t_i approach the Gauss-Legendre point (cf. (4.33)) as $\rho_i \to 0$. When ρ_i is large $t_i \simeq (1/\rho_i)\ln(\rho_i/2)$ and in this case (3.12), (4.18), and (4.23) imply that

$$S_i \simeq \gamma_i \hat{p}_i(1)/\rho_i^* \quad . \tag{4.28}$$

The computational evidence in Section 5 indicates that S_i is not small enough to insure an accurate approximation of $e'(x_j)$ at any knot point. In fact, the indications are that $e(x_j) \simeq 0(h^2)$ while $e'(x_j) \simeq 0(h^2/\varepsilon)$ when ρ_i is large. Method 2 may still be used in this case if one is not interested in predicting the slope of the

solution as long as ρ_i is not so large that it causes the discrete system (2.18-20) to be ill-conditioned. When ρ_i is small t_i approaches the Gauss-Legendre point and $e(x_j)$ and $e'(x_j)$ will approach $0(h^4)$ (cf. deBoor and Swartz [8]).

For polynomial approximations, we use (4.8) in (4.19) to get

$$S_i \simeq \int_0^1 e^{-\rho_i^*(1-s)} (s-t_i)(s-1+t_i)\hat{r}_i[t_i,1-t_i,s]ds \quad , \tag{4.29a}$$

$$R_i = \int_0^1 \hat{\zeta}_i(s)(s-t_i)(s-1+t_i)\hat{r}_i[t_i,1-t_i,s]ds \quad , \tag{4.29b}$$

where, once again, Laplace's method was used to approximate the singular integral S_i.

Either S_i or R_i may be reduced in magnitude by selecting t_i such that either $e^{-\rho_i^*(1-s)}$ or 1 is orthogonal to $(s-t_i)(s-1+t_i)$, respectively, i.e., by requiring either

$$\int_0^1 e^{-\rho_i^*(1-s)} (s-t_i)(s-1+t_i)ds = 0 \quad \text{or} \quad \int_0^1 (s-t_i)(s-1+t_i)ds = 0 \; . \tag{4.30a,b}$$

The option (4.30a) gives

$$t_i = \frac{2}{\rho_i^*} \; \frac{\omega(\rho_i^*/2)}{1+\sqrt{1-4\omega(\rho_i^*/2)/\rho_i^*}} \tag{4.31}$$

where $\omega(z)$ was defined in (2.12). This method is referred to as Method 3. Once again, t_i approaches the Gauss-Legendre point as $\rho_i \to 0$ and $t_i \simeq 1/\rho_i^*$ when ρ_i is large. Assuming that y_h and y_h' are bounded outside of the boundary layer region and using (4.4b) and Taylor's series expansions of $f(x)$ and $Ly_h(x)$ about x_i in (4.29b) leads to

$$R_i \simeq -\frac{h^2}{12} \hat{\zeta}_i(1)[f(x_i) - Ly_h(x_i)]'' \quad . \tag{4.32}$$

This in turn via (4.16) would imply that $e(x_j)$ and $e'(x_j)$ are $0(h^2)$ at knot points outside of the boundary layer. However, it is typically possible to replace $(Ly_h(x_j))''$ by $(Ly(x_j))'' + 0(h)$ (cf. Pruess [21] or Russell and Christiansen [24]). If this were so, this R_i, $e(x_j)$, and $e'(x_j)$ would all be $0(h^3)$ at knots away from the boundary layer. This is in accord with the computational results of Section 5.

The final possibility is to select t_i so that (4.30b) is zero and this gives t_i as the Gauss-Legendre point on the interval [0,1], i.e.,

$$t_i = (1 - 1/\sqrt{3})/2 \ . \tag{4.33}$$

This choice of t_i is known to give poor results when $hp(x)/\varepsilon >> 1$; however, in Section 5, we show that it may be used outside of subintervals containing boundary layers provided that y_h and y_h' are computed accurately enough at the ends of subintervals containing boundary layers.

4.3. Collocation Points for Problem 2

Again, let x be a knot point, say x_j, and use (3.9) and (4.3) to write

$$\Pi(x_{i-1}+hs,x_j) = \Pi(x_i,x_j)\hat{\pi}_i(s) = \delta_{ij}\hat{\pi}(s) \ , \quad i \le j \tag{4.34a}$$

$$\Pi(x_j,x_i+hs) = \Pi(x_j,x_i)\hat{\lambda}_i(s) = \delta_{ij}\hat{\lambda}_i(s) \ , \quad i \ge j \ , \tag{4.34b}$$

where now

$$\hat{\pi}_i(s) = \exp\{-h\int_s^1 \sqrt{-\hat{q}_i(s)/\varepsilon}\,ds\}, \ \hat{\lambda}_{i+1}(s) = \exp\{-h\int_0^s \sqrt{-\hat{q}_{i+1}(s)/\varepsilon}\,ds \ . \tag{4.34c,d}$$

The last forms of (4.34) again follow from our assumption that terms of $0(e^{-\rho_i/2})$ are negligible. Using (3.11) and (4.34) in (4.7) we have

(4.35a) $$e(x_j) = \frac{h}{2}\left(\delta_{0j}\,\tilde{S}_1 + \delta_{Nj}\,S_N - S_j - \tilde{S}_{j+1}\right),$$

(4.35b) $$e'(x_j) = \frac{h}{2}\left[-\left(\rho_0^*/h + q_0'/q_0\right)\delta_{0j}\,\tilde{S}_1 + \left(\rho_N^*/h - q_N'/q_N\right)\delta_{Nj}\,S_N + \left(\rho_j^*/h + q_j'/q_j\right)S_j - \left(\rho_j^*/h - q_j'/q_j\right)\tilde{S}_{j+1}\right],$$

where

(4.36a,b) $$q_j = q(x_j), \quad \rho_j^* = h\sqrt{-q(x_j)/\varepsilon},$$

and

(4.37a) $$S_j = \int_0^1 \hat{\pi}_j(s)\left[\varepsilon^2 q(x_j)\hat{q}_j(s)\right]^{-1/4}(1-P)\hat{r}_j(s)\,ds,$$

(4.37b) $$\tilde{S}_{j+1} = \int_0^1 \hat{\lambda}_{j+1}(s)\left[\varepsilon^2 q(x_j)\hat{q}_j(s)\right]^{-1/4}(1-P)\hat{r}_{j+1}(s)\,ds.$$

Thus, in this problem, there are no regular integrals to consider.

It suffices to find collocation points for S_j since analogous results for $\tilde{S}_{j+1}$ will follow by replacing s by 1-s and making the appropriate sign changes in (4.37b). Thus, using Laplace's method we approximate (4.37a) by

(4.38) $$S_j \simeq \int_0^1 e^{-\rho_j^*(1-s)}\left[\varepsilon^2 q(x_j)\hat{q}_j(s)\right]^{-1/4}(1-P)\hat{r}_j(s)\,ds.$$

For taut spline approximations, the choice of ρ_j given by (3.13b) reduces both $\hat{u}_j(s)$ and $\hat{v}_j(s)$ (cf. (4.11)) to $0(h^2/\rho_j)$ and it is still reasonable to select t_j according to (4.25), i.e., so that (4.24) is satisfied with ρ_j and ρ_j^* given by (3.13b) and (4.36b), respectively. We continue to refer to this choice of t_j as Method 1. Likewise, for polynomial approximations, we select t_j according to (4.31), i.e., so that (4.30a) is satisfied, and still refer to this as Method 3. Both methods reduce S_j (hence, $\tilde{S}_{j+1}$) to at least $0(ht_j)$. Since t_j is $0(1/\rho_j)$ or $0(1/\rho_j^*)$ for Method 1 or 3, respectively, and h/ρ_j and h/ρ_j^* are both $0(\sqrt{\varepsilon})$

(cf. (3.13b) and (4.36b)), we would expect (cf. (4.35a)) $e(x_j)$ to be at most $0(h\sqrt{\varepsilon})$ at knots away from boundary layers. The computational results of Section 5 support this conclusion.

5. Numerical Results

In this section, we apply Methods 1, 2, and 3 of Section 4 to three examples having known exact solutions. Our calculations are performed on a uniform partition with spacing h and the adjoint tension parameters ρ_j^* are approximated as

$$\rho_j^* = h \begin{cases} |p(x_k)/\varepsilon - q(x_k)/p(x_k)|, & |\mu p(x_j)/\varepsilon| \geq |\mu q(x_j)| \\ \sqrt{-\mu q(x_j)/2\varepsilon}, & |\mu p(x_j)/\varepsilon| < |\mu q(x_j)| \end{cases} \tag{5.1a}$$

$$j = 1,2,\ldots,N,$$

where

$$k = \begin{cases} j-1 & \text{if } \mu p(x_j)/\varepsilon < 0 \\ j & \text{if } \mu p(x_j)/\varepsilon > 0 \end{cases} \tag{5.1b}$$

The tension parameters ρ_j and collocation points t_j on I_j are chosen as follows:

Method 1: Select ρ_j according to (3.12) and

$$t_j = \min\{(1/\rho_j)\ \ln\ (1+\rho_j/\rho_j^*)\ ,\ (1-1/\sqrt{3})/2\} \tag{5.2a}$$

Method 2: Select ρ_j according to (3.12) and

$$t_j = \frac{1}{2}\left[1 - \frac{2}{\rho_j}\cosh^{-1}\left(\frac{2}{\rho_j}\sinh\frac{\rho_j}{2}\right)\right] \tag{5.2b}$$

Method 3: Select $\rho_j = 0$ and

$$t_j = \frac{2}{\rho_j^*}\,\frac{\omega(\rho_j^*/2)}{1+\sqrt{1-4\omega(\rho_j^*/2)/\rho_j^*}} \tag{5.2c}$$

We also consider "partial tension" methods where the above rules for selecting ρ_j and t_j are only applied on subintervals containing boundary layers and collocation is performed at the

Gauss-Legendre point with $\rho_j = 0$ on all other subintervals. These methods can potentially converge as $0(h^4)$ outside of boundary layer subintervals provided that the numerical solution and its derivative have been computed accurately enough at the ends of subintervals containing boundary layers. Thus, we would not expect partial tension to be useful with Method 2 since there can be large errors in the derivative of the computed solution at the knots. We denote the partial tension methods that use either Method 1 or 3 within boundary layer subintervals as either Method 1P or 3P, respectively. In order to automatically locate subintervals containing boundary layers we first compute a preliminary solution, c_j^0, d_j^0, $j=0,1,\ldots,N$ using either Method 1 or 3 on all subintervals. Using this solution we calculate

$$\bar{y}_j'' = |\mu[f(x_j)-p(x_j)d_j^0-q(x_j)c_j^0]/2\varepsilon , \quad j=1,2,\ldots,N . \tag{5.3}$$

and set $\rho_j = 0$ and $t_j = (1-1/\sqrt{3})/2$ on any subinterval having

$$\bar{y}_j'' < \delta \min\{1,\bar{y}_i'',\bar{y}_2'',\ldots,\bar{y}_N''\} , \tag{5.4}$$

where δ is a threshold constant which we normally take as 50. The problem is then re-solved using the new values of ρ_j and t_j. This procedure is somewhat ad hoc and has not been totally effective, especially when h is relatively large and c_j^0 and d_j^0 are inaccurate. This can cause errors in $\bar{y}_j''$ which can lead to the erroneous conclusion that a subinterval contains a boundary layer when in fact it does not, and vice versa.

Each example was solved for various values of ε and $h = (b-a)/N$ with $N = 2^k$, $k = 2,3,\ldots,7$. The error in the solution and its derivative on a partition with spacing h are measured by

$$||e^{(i)}||_{h,\Delta_0} \equiv \max_{x_j\varepsilon\Delta_0} |y^{(i)}(x_j) - y_h^{(i)}(x_j)| \qquad i = 0,1 \tag{5.5}$$

where Δ_0 is a fixed uniform partition that is specified with each example. The order of convergence r_i is computed as

$$r_i = \ln \{||e^{(i)}||_{h,\Delta_0} / ||e^{(i)}||_{h/2,\Delta_0}\} / \ln 2 \quad , \quad i = 0,1 \ . \tag{5.6}$$

All calculations were performed in double precision on an IBM 3033 computer. Errors that are less than 5×10^{-15} are recorded as zero in the tables.

Example 1:

$$\begin{aligned} &\varepsilon y'' + ((1+x)y)' = e^{-x/2}\,[(1+x)(3-x)+\varepsilon/2]/2 \ , \quad 0 < x < 1 \ , \\ &y(0) = 0 \quad , \quad y(1) = e^{-1/2} - e^{-7/3\varepsilon} \end{aligned} \tag{5.7}$$

The exact solution of this problem is

$$y(x) = \exp(-x/2) - \exp[-x(x^2+3x+3)/3\varepsilon] \ .$$

There is a boundary layer of width $0(\varepsilon)$ near $x = 0$.

In order to demonstrate how poorly collocation at the Gauss-Legendre points with cubic polynomials can behave on singularly-perturbed problems, we solved (5.7) with $\varepsilon = 10^{-4}$ and $h = 1/8$ by this method and plotted the computed solution in Figure 2. It bears little resemblance to the exact solution which is essentially $e^{-x/2}$ for $x > 10^{-3}$. Pointwise the numerical solution approximately lies on the straight line joining the two boundary values $y(0)$ and $y(1)$.

We solved (5.7) for $\varepsilon = 10^{-i}$, $i = 2,4,6,8$ using Methods 1, 2, 3, and 1P. The errors $||e||_{h,\Delta_0}$ and $||e'||_{h,\Delta_0}$ on the partition $\Delta_0 = \{1/8, 1/4, 3/8, \ldots, 7/8\}$ are presented in Tables 1 and 2, respectively, for $\varepsilon = 10^{-2}$, 10^{-4}, and 10^{-8}. (The results for $\varepsilon = 10^{-6}$ were essentially the same as those for 10^{-8}.) $||e||_{h,\Delta_0}$ is also plotted as a function of $1/h$ in Figure 3 for Methods 1, 2,

and 3 and $\varepsilon = 10^{-i}$, i=2,4,6,8. Tables 1 and 2 indicate that when $\varepsilon/h << 1$, Methods 1, 2, and 3 are converging as $0(h)$, $0(h^2)$, and $0(h^3)$, respectively, and that $||e'||_{h,\Delta_0}$ is converging as $0(h^2/\varepsilon)$ for Method 2. For larger values of ε, e.g. $\varepsilon = 10^{-2}$, the order of convergence can be seen to increase as h decreases (ε/h increases) and the collocation points move closer to the Gauss-Legendre points. Partial tension with Method 1P yields a dramatic improvement in the results obtained by Method 1.

In order to provide some indication of how Methods 1, 2, and 3 behave on subintervals containing boundary layers and between knot points, we have plotted their computed solutions $y_h(x)$ on $0 \leq x \leq 2h$ (Figure 4) and their errors $e(x)$ and $e'(x)$ on $0 \leq x \leq 1$ (Figures 5,6,7) for $\varepsilon = 10^{-4}$ and $h = 1/8$. The error in the Method 2 solution shown in Figure 4 is less than 3.2×10^{-3} for all $x \in I_1 \cup I_2$. Method 1 yields poor accuracy for $x \in I_1$, but it does predict the correct width of the boundary layer. Method 3 dissipates the boundary layer; however, the dissipation is largely confined the subinterval I_1 containing the boundary layer. Figures 5-7 show that all three methods have spurious internal boundary layer jumps in $y_h'(x)$ at the ends of each subinterval and that Method 2, because of the singular behavior of y_h' in ε at the knots, has spurious jumps in $y_h(x)$ itself. The jumps in $y_h(x)$ are small and one is not normally interested in the solution at points other than the knot points; however, the results indicate that some caution is needed when using (2.7-12) to interpolate the solution between knot points.

Figures 5-7 further indicate that the pointwise error is largest at $x_1 = h$ and decreases at knots that are farther from

the boundary layer. This is generally true for other values of h as well and, thus, we have tabulated $|e(h)|$ for Methods 1, 2, and 3 with $\varepsilon = 10^{-i}$, $i = 2,4,6,8$ and $N = 2^i$, $i = 2,3,\ldots,7$, in Table 3. The results for Methods 2 and 3 indicate that $|e(h)|$ cannot be reduced below $0(\varepsilon)$ until ε/h^2 and ε/h^3, respectively, are sufficiently small.

Example 2:

$$\varepsilon^2 y'' - (x^2+\varepsilon)y = -(x^2+\varepsilon)(1+\sin \pi x) - \varepsilon^2\pi^2 \sin \pi x, \quad 0 < x < 1 , \tag{5.8}$$

$$y(0) = y(1) = 0 .$$

The exact solution of this example is

$$y(x) = 1 + \sin \pi x - \frac{1}{\operatorname{erf}(\sqrt{1/\varepsilon})} \{(1-e^{-1/2\varepsilon})W(x/\sqrt{\varepsilon})e^{-x^2/2\varepsilon}$$

$$+ [1-e^{-1/2\varepsilon}W(\sqrt{1/\varepsilon})]e^{-(1-x^2)/2\varepsilon}\} ,$$

where

$$W(z) = e^{z^2}\operatorname{erfc}(z) .$$

(Note that y'' is multiplied by ε^2 instead of ε for notational simplicity.) The exact solution of (5.8) has a boundary layer of width $0(\sqrt{\varepsilon})$ near $x = 0$ and one of width $0(\varepsilon)$ near $x = 1$. This problem does not satisfy the assumptions of Problem 2 since $q(x) = -(x^2+\varepsilon)$ cannot be bounded away from zero at $x = 0$ as $\varepsilon \to 0$; thus, $x = 0$ is a turning point.

We computed solutions by Methods 1 and 3 for $\varepsilon = 10^{-i}$, $i=2,4,6,8$. Solutions were also calculated using the collocation points of Method 3 (cf. (5.2c)) but with splines under tension instead of polynomial splines, and these are denoted as Method 3T. The errors $||e||_{h,\Delta_0}$ and $||e'||_{h,\Delta_0}$ are presented in Tables 4 and 5, respectively, for the partition $\Delta_0 = \{1/8, 1/4, 3/8,\ldots,7/8\}$. Partial Tension

solutions using Methods 1 and 3T were also calculated and the results were marginally more accurate than those of Method 1.

Tables 4 and 5 indicate that when $\varepsilon/h << 1$, $||e||_{h,\Delta_0}$ and $||e'||_{h,\Delta_0}$ are $0(\varepsilon h)$ and $0(h^2)$, respectively, for Method 1 and $0(\varepsilon h^3)$ and $0(h^2)$, respectively, for Method 3T. The small errors in Method 3 make it difficult to estimate the order of convergence.

The largest error on the partition $\Delta = \{0,h,2h,\ldots,Nh = 1\}$ used for the computation was once again at the end of a subinterval containing a boundary layer, i.e., either at $x_1 = h$ or $x_{N-1} = (N-1)h$. To indicate how this error behaves, we present results for $||e||_{h,\Delta}$ in Table 6. For small values of ε/h we see that the polynomial solution (Method 3) is not converging in h and that this situation is remedied by using taut splines (Method 3T). Although we have not done so, we suspect that it would have been sufficient to use taut splines only within subintervals containing boundary layers. Furthermore, Methods 1 and 3 do not appear to be uniformly convergent in h for all ε. All methods are converging as $0(\varepsilon)$ which accounts for the remarkable accuracy when ε is small.

Example 3: (cf. Hemker [15])

$$\varepsilon y'' + xy' = -\varepsilon\pi^2 \cos \pi x - \pi x \sin \pi x \quad , \quad -1 < x < 1 \ , \tag{5.9}$$

$$y(-1) = -2 \quad , \quad y(1) = 0 \ .$$

The exact solution of this example is

$$y(x) = \cos \pi x + \operatorname{erf}\,(x/\sqrt{2\varepsilon})/\operatorname{erf}\,(1/\sqrt{2\varepsilon}) \ .$$

The problem has a turning point at $x = 0$ and the exact solution features an interior or "shock" layer there.

Solutions were calculated by Methods 1, 2, 3, and 1P for $\varepsilon = 10^{-i}$, i=2,4,6,8. The errors $||e||_{h,\Delta_0}$ and $||e'||_{h,\Delta_0}$ on the

partition $\Delta_0 = \{-3/4, -1/2, -1/4, 1/4, 1/2, 3/4\}$ are presented in Tables 7 and 8, respectively for $\varepsilon = 10^{-2}$, 10^{-4}, and 10^{-8}. (The results for $\varepsilon = 10^{-6}$ were essentially the same as those for $\varepsilon = 10^{-8}$.) The results for $||e||_{h,\Delta_0}$ are indicating the same orders of convergence as found in Example 1; however, for Methods 1 and 3, $||e'||_{h,\Delta_0}$ is much more accurate than the corresponding values for example 1.

In order to include the behavior of the solution in the turning point region, we have tabulated $||e||_{h,\Delta}$ on the partition $\Delta = \{-1,-1+h,\ldots,-1+Nh=1\}$ used for the calculation in Table 9. Note that $||e||_{h,\Delta_0} = ||e||_{h,\Delta}$ for Method 1, so the maximum error is not in the turning point region. Methods 2 and 3 are both exhibiting regions of non-uniform convergence in h.

6. *Discussion and Conclusions*

Based on the results of Sections 4 and 5, we conclude that splines under tension are most suitable in regions containing boundary and/or interior layers and that collocation with piecewise polynomials are superior elsewhere. In particular, when $\varepsilon/h << 1$ Method 3 provides an approximation that converges outside of boundary layer subintervals as $0(h^3)$ when $p(x) \neq 0$ and at least $0(\sqrt{\varepsilon}h)$ when $p(x) \equiv 0$ on $[a,b]$. Hemker [15] and de Groen and Hemker [10] reached similar conclusions with their exponentially fitted Galerkin methods.

Partial tension can converge as $0(h^4)$ outside of boundary layer subintervals, but either requires a knowledge of boundary layer locations or a preliminary solution to automatically locate them. The latter procedure may be useful for nonlinear problems

where it is necessary to solve a sequence of linear problems to find the solution; however, for linear problems it does not seem to warrant the extra computational effort merely to obtain one order of accuracy more than that available by Method 3.

The use of "one sided splines under tension," i.e., the selection of basis functions that satisfy

$$(\eta' + \rho\eta)''' = 0 \quad , \quad 0 < s < 1 \, , \tag{6.1}$$

instead of (2.14) would undoubtably improve the results on subintervals where $p(x) \neq 0$. A basis for these approximations would contain either the exponential $\exp(-\rho s)$ when $\rho > 0$ or $\exp(-|\rho|(1-s))$ when $\rho < 0$, and not both as in the current case. This would more accurately represent the exact solution of problems where $p(x) \neq 0$ on $[a,b]$. The results could possibly be further improved by not restricting the collocation points to be placed symmetrically on each subinterval and by using non-uniform partitions. Each of these potential improvements is currently under investigation. Extensions of our methods to higher order scalar and vector systems of two-point boundary value problems as well as second order parabolic partial differential equations are also being studied.

Acknowledgement.

The authors would like to thank Professors G. J. Habetler and R. E. O'Malley, Jr., for their valuable comments and suggestions and Mr. G. M. Heitker for his assistance with some of the programming.

References

[1] L. R. Abrahamson, H. B. Keller, and H. O. Kreiss, Difference approximations for singular perturbations of systems of ordinary differential equations, Numer. Math., 22 (1974), pp. 367-391.

[2] U. Ascher, J. Christiansen, and R. D. Russell, Collocation software for boundary value ODE's, preprint, 1979.

[3] C. M. Bender and S. A. Orszag, Advanced Mathematical Methods for Scientists and Engineers, McGraw Hill, New York, 1978.

[4] A. E. Berger, J. M. Solomon, and M. Ciment, Higher order accurate tridiagonal difference methods for diffusion convection equations, to appear in Proc. Third IMACS Conf. on Computer Meths. for Partial Differential Eqns., Lehigh Univ., 1979.

[5] A. Cline, Curve fitting in one and two dimensions using Splines under tension, CACM, 17 (1974), pp. 218-223.

[6] J. Cole, Perturbation Methods in Applied Mathematics, Blaisdell Publishing Co., Waltham, Mass., 1968.

[7] M. J. Coyle and J. E. Flaherty, The solution of boundary value problems having rapidly oscillating solutions, in preparation.

[8] C. de Boor and B. Swartz, Collocation at Gaussian points, SIAM J. Numer. Anal., 10 (1973), pp. 582-607.

[9] C. de Boor, A Practical Guide to Splines, Applied Mathematical Sciences 27, Springer Verlag, New York, 1978.

[10] P. P. N. de Groen and P. W. Hemker, Error bounds for exponentially fitted Galerkin methods applied to stiff two-point boundary value problems, in Numerical Analysis of Singular Perturbation

Problems, P. W. Hemker and J. J. H. Miller, Eds., Academic Press, London, 1979.

[11] W. Eckhaus, Matched Asymptotic Expansions and Singular Perturbations, North-Holland Mathematics Studies 6, North-Holland, Amsterdam, 1973.

[12] J. E. Flaherty and R. E. O'Malley, Jr., The numerical solution of boundary value problems for stiff differential equations, Maths. Comp., 31 (1977), pp. 66-93.

[13] J. C. Heinrich, P. S. Huyakorn, O. C. Zienkiewicz, and O. R. Mitchell, An upwind finite element scheme for two-dimensional convective transport equation, Int. J. Numer. Meths. Engr., 11 (1977), pp. 131-143.

[14] J. C. Heinrich and O. C. Zienkiewicz, Quadratic finite element schemes for two dimensional convective-transport problems, Int. J. Numer. Meths. Engr., 11 (1977), pp. 1831-1844.

[15] P. W. Hemker, A numerical study of stiff two-point boundary problems, Ph.D. Dissertation, Mathematisch Centrum, Amsterdam, 1977.

[16] A. M. Il'in, Differencing scheme for a differential equation with a small parameter affecting the highest derivative, Math. Notes Acad. Sc. USSR, 6 (1969), pp. 596-602.

[17] H. O. Kreiss, Difference approximations for singular perturbation problems, Numerical Solutions of Boundary Value Problems for Ordinary Differential Equations, A. K. Aziz, Ed., Academic Press, 1975, pp. 199-212.

[18] R. E. O'Malley, Jr., Introduction to Singular Perturbation, Academic Press, New York, 1979.

[19] C. E. Pearson, On a differential equation of the boundary layer type, J. Math. and Physics, 47 (1968), pp. 134-154.

[20] C. E. Pearson, On nonlinear ordinary differential equations of boundary layer type, J. Math. and Physics, 47 (1968), pp. 351-358.

[21] S. A. Pruess, Solving linear boundary value problems by approximating the coefficients, Math. Comp., 27 (1973), pp. 551-561.

[22] S. Pruess, Properties of splines in tension, J. Approx. Th., 17 (1976), pp. 86-96.

[23] R. D. Russell, Collocation for systems of boundary value problems, Numer. Math., 23 (1974), pp. 119-133.

[24] R. D. Russell and J. Christiansen, Adaptive mesh selection strategies for solving boundary value problems, SIAM J. Numer. Anal., 15 (1978), pp. 59-80.

[25] R. D. Russell and L. F. Shampine, A collocation method for boundary value problems, Numer. Math., 19 (1972), pp. 1-28.

[26] D. Schweikert, An interpolation curve using splines in tension, J. Math. Phys., 45 (1966), pp. 312-317.

[27] H. Späth, Spline-Algorithmen zur Konstruktion glatter Kurven und Flächen, R. Oldenbourg Verlag, München, 1973. English translation by W. D. Hoskins and H. W. Sager, Spline Algorithms for Curves and Surfaces, Utilitas Mathematica, Winnipeg, 1974.

[28] G. V. Ranjan and C. R. Steele, Analysis of knuckle region between two smooth shells, J. Appl. Mech., 42 (1974), pp. 853-857.

[29] J. M. Varah, Alternate row and column elimination for solving certain linear systems, SIAM J. Numer. Anal., 13 (1976), pp. 71-75.

[30] W. Wasow, Asymptotic Expansions for Ordinary Differential Equations, Wiley-Interscience, New York, 1965.

METHOD	N	$\epsilon = 10^{-2}$		10^{-4}		10^{-8}	
		$\|\|e\|\|_{h,\Delta_0}$	r_0	$\|\|e\|\|_{h,\Delta_0}$	r_0	$\|\|e\|\|_{h,\Delta_0}$	r_0
1	4	3.87E-2		4.63E-2		4.37E-2	
	8	1.95E-2	1.0	2.44E-2	0.8	2.44E-2	0.8
	16	7.06E-3	1.5	1.09E-2	1.2	1.09E-2	1.2
	32	2.02E-3	1.8	5.15E-3	1.1	5.15E-3	1.1
	64	2.50E-4	3.0	2.49E-3	1.0	2.53E-3	1.0
	128	5.69E-6	5.5	1.21E-3	1.0	1.25E-3	1.0
2	4	2.34E-2		2.09E-3		1.28E-3	
	8	1.28E-2	0.9	1.13E-3	0.9	4.40E-4	1.5
	16	1.07E-4	6.9	9.59E-5	3.6	1.07E-4	2.0
	32	3.34E-5	1.7	2.14E-5	2.2	2.63E-5	2.0
	64	4.83E-6	2.8	4.41E-6	2.3	6.50E-6	2.0
	128	4.37E-7	3.5	7.39E-7	2.6	1.62E-6	2.0
3	4	4.37E-3		3.57E-5		1.34E-5	
	8	3.70E-3	0.2	5.56E-5	-0.6	1.77E-6	2.9
	16	5.79E-7	12.6	2.76E-7	7.7	1.99E-7	3.2
	32	5.92E-8	3.3	3.37E-8	3.0	3.38E-8	2.6
	64	1.93E-9	4.9	4.19E-9	3.0	4.23E-9	3.0
	128	6.43E-11	4.9	5.19E-10	3.0	5.37E-10	3.0
1P	4	2.67E-6		3.69E-7		1.10E-2	
	8	1.06E-6	1.3	3.38E-8	3.4	3.29E-8	18.4
	16	4.64E-6	-2.1	1.86E-9	4.2	2.05E-9	4.0
	32	2.12E-6	1.1	2.64E-11	6.1	1.33E-10	6.0
	64	9.11E-8	4.5	5.89E-11	-1.2	8.68E-12	3.9
	128	4.68E-9	4.3	1.78E-11	1.7	6.24E-13	3.8

Table 1: Error and Order of Convergence for Example 1 Measured on $\Delta_0 = \{1/8, 1/4, 3/8, \ldots, 7/8\}$.

METHOD	N	$\varepsilon = 10^{-2}$		10^{-4}		10^{-8}	
		$\|\|e'\|\|_{h,\Delta_0}$	r_1	$\|\|e'\|\|_{h,\Delta_0}$	r_1	$\|\|e'\|\|_{h,\Delta_0}$	r_1
1	4	6.38E-2		6.97E-2		6.99E-2	
	8	3.54E-2	0.8	4.34E-2	0.7	4.35E-2	0.7
	16	1.22E-2	0.3	1.93E-2	1.2	1.94E-2	1.2
	32	3.14E-3	2.0	9.15E-3	1.1	9.22E-3	1.1
	64	1.15E-4	4.8	4.43E-3	1.0	4.50E-3	1.0
	128	8.09E-5	0.5	2.15E-3	1.0	2.22E-3	1.0
2	4	4.14E 0		1.01E-2		1.01E 6	
	8	1.75E 0	1.2	2.43E-1	2.1	2.45E 5	2.0
	16	3.84E-2	2.2	5.58E 0	2.1	6.02E 4	2.0
	32	6.64E-3	2.5	1.37E 0	2.0	1.49E 4	2.0
	64	8.24E-4	3.0	3.38E-1	2.0	3.72E 3	2.0
	128	7.10E-5	3.5	8.24E-2	2.0	9.27E 2	2.0
3	4	3.05E-3		5.68E-5		2.14E-5	
	8	1.99E-2	-2.7	9.62E-5	-0.8	3.14E-6	2.8
	16	8.65E-5	7.8	4.90E-7	7.6	3.18E-7	3.3
	32	1.92E-5	5.2	6.00E-8	3.0	6.01E-8	2.4
	64	1.37E-6	3.8	7.44E-9	3.0	7.53E-9	3.0
	128	9.56E-8	3.8	9.23E-10	3.0	9.54E-10	3.0
1P	4	9.18E-4		6.08E-5		1.76E-2	
	8	1.41E-4	2.7	2.41E-5	1.3	2.19E-5	9.7
	16	5.86E-4	1.3	6.46E-6	1.9	5.48E-6	2.0
	32	2.68E-4	1.1	7.33E-7	3.1	1.52E-6	1.9
	64	1.15E-5	4.5	8.11E-7	-0.1	4.25E-7	1.8
	128	5.93E-7	4.3	2.18E-7	1.9	1.46E-7	1.5

Table 2: Error and Order of Convergence in the Derivative of the Solution of Example 1 Measured on $\Delta_0 = \{1/8, 1/4, 3/8, \ldots, 7/8\}$.

METHOD	N	$\varepsilon = 10^{-2}$		10^{-4}		10^{-6}		10^{-8}	
		e(h)	r	e(h)	r	e(h)	r	e(h)	r
1	4	3.87E-2		4.36E-2		4.37E-2		4.37E-2	
	8	1.95E-2	1.0	2.44E-2	0.8	2.45E-2	0.8	2.44E-2	0.8
	16	7.89E-3	1.3	1.28E-2	0.9	1.29E-2	0.9	1.29E-2	0.9
	32	2.25E-3	1.8	6.57E-3	1.0	6.62E-3	1.0	6.62E-3	1.0
	64	3.08E-4	2.9	3.30E-3	1.0	3.35E-3	1.0	3.35E-3	1.0
	128	6.23E-6	5.6	1.63E-3	1.0	1.69E-3	1.0	1.69E-3	1.0
2	4	2.34E-2		2.09E-3		1.30E-3		1.28E-3	
	8	1.28E-2	0.9	1.13E-3	0.9	4.52E-4	1.5	4.40E-4	1.5
	16	4.19E-3	1.6	7.15E-4	0.7	1.36E-4	1.3	1.26E-4	1.8
	32	2.47E-4	4.1	5.39E-4	0.4	4.32E-5	1.7	3.35E-5	1.9
	64	4.45E-5	2.5	4.36E-4	0.3	1.76E-5	1.3	8.72E-6	1.9
	128	5.48E-6	3.0	3.51E-4	0.3	1.05E-5	0.7	2.31E-6	1.5
3	4	4.37E-3		3.57E-5		1.28E-5		1.34E-5	
	8	3.70E-3	0.2	5.56E-5	-0.6	1.62E-6	3.0	1.77E-6	2.9
	16	1.38E-3	1.4	6.17E-5	-0.2	3.35E-7	2.3	3.04E-7	2.5
	32	7.65E-4	0.9	6.34E-5	-0.0	8.50E-7	-1.3	2.99E-8	1.1
	64	8.48E-5	3.2	6.29E-5	0.0	7.13E-7	0.3	2.99E-8	0.0
	128	4.39E-6	4.3	6.05E-5	0.1	6.79E-7	0.1	3.61E-7	-3.6

Table 3: Error at the Knot Point x_1 for Example 1.

METHOD	N	$\varepsilon = 10^{-2}$		10^{-4}		10^{-6}		10^{-8}	
		$\|\|e\|\|_{h,\Delta_0}$	r_0	$\|\|e\|\|_{h,\Delta_0}$	r_0	$\|\|e\|\|_{h,\Delta_0}$	r_0	$\|\|e\|\|_{h,\Delta_0}$	r_0
1	4	7.35E-3		1.54E-4		1.57E-6		1.57E-8	
	8	3.83E-3	0.9	8.75E-5	0.8	9.19E-7	0.8	9.21E-9	0.8
	16	3.99E-4	3.3	3.05E-5	1.5	3.24E-7	1.5	3.24E-9	1.5
	32	4.67E-5	3.1	1.30E-5	1.8	1.49E-7	1.1	1.49E-9	1.1
	64	3.20E-6	3.9	5.84E-6	1.2	7.28E-8	1.0	7.30E-10	1.0
	128	2.05E-7	4.0	2.50E-6	1.2	3.61E-8	1.0	3.63E-10	1.0
3	4	3.13E-2		4.66E-4		4.67E-6		4.67E-8	
	8	2.93E-2	0.1	5.92E-4	-0.3	5.95E-6	-0.3	5.96E-8	-0.4
	16	3.42E-4	6.4	9.92E-7	9.2	1.02E-10	15.8	1.04E-14	22.5
	32	4.58E-6	6.2	5.97E-10	10.7	1.00E-13	10.0	0.0	
	64	2.87E-7	4.0	1.57E-10	1.9	2.46E-14	2.0	0.0	
	128	1.80E-8	4.0	2.37E-11	2.7	6.00E-15	2.0	0.0	
3T	4	4.93E-3		8.55E-5		8.65E-7		8.65E-9	
	8	1.05E-3	2.2	4.85E-5	0.8	5.06E-7	0.8	5.06E-9	0.8
	16	8.70E-5	3.6	3.84E-6	3.7	3.94E-8	3.7	3.94E-10	3.7
	32	5.76E-6	3.9	4.73E-7	3.0	4.88E-9	3.0	4.88E-11	3.0
	64	3.66E-7	4.0	5.74E-8	3.0	6.08E-10	3.0	6.09E-11	3.0
	128	2.29E-8	4.0	6.66E-9	3.1	7.60E-11	3.0	7.61E-13	3.0

Table 4: Error and Order of Convergence for Example 2 Measured on $\Delta_0 = \{1/8, 1/4, 3/8, \ldots, 7/8\}$.

METHOD	N	$\varepsilon = 10^{-2}$		10^{-4}		10^{-6}		10^{-8}	
		$\|\|e'\|\|_{h,\Delta_0}$	r_1	$\|\|e'\|\|_{h,\Delta_0}$	r_1	$\|\|e'\|\|_{h,\Delta_0}$	r_1	$\|\|e'\|\|_{h,\Delta_0}$	r_1
1	4	1.36E-1		2.81E-1		2.79E-1		2.78E-1	
	8	2.68E-2	2.3	8.65E-2	1.7	8.76E-2	1.7	8.76E-2	1.7
	16	4.46E-3	2.6	2.37E-2	1.9	2.49E-2	1.8	2.49E-2	1.8
	32	1.43E-4	5.0	5.88E-3	2.0	6.45E-3	1.9	6.46E-3	1.9
	64	8.35E-6	4.1	1.36E-3	2.1	1.63E-3	2.0	1.64E-3	2.0
	128	5.10E-7	4.0	3.02E-4	2.2	4.07E-4	2.0	4.09E-4	2.0
3	4	2.04E 0		2.97E 0		2.97E 0		2.98E 0	
	8	2.37E 0	-0.2	4.82E 0	-0.7	4.85E 0	-0.7	4.85E 0	-0.7
	16	2.87E-2	6.4	8.37E-3	9.2	3.93E-8	26.9	8.40E-7	22.5
	32	4.12E-5	9.4	6.34E-7	10.4	4.09E-9	3.3	2.72E-8	4.9
	64	2.13E-5	1.0	3.78E-8	4.1	4.86E-10	3.1	2.74E-8	0.0
	128	1.34E-6	4.0	3.48E-9	3.4	9.52E-11	2.4	2.59E-8	0.1
3T	4	1.10E-1		2.01E-1		2.02E-1		2.02E-1	
	8	1.45E-2	2.9	7.31E-2	1.5	7.45E-2	1.4	7.45E-2	1.4
	16	5.18E-4	4.8	1.89E-2	2.0	2.04E-2	1.9	2.04E-2	1.9
	32	1.25E-4	2.1	4.63E-3	2.0	5.33E-3	1.9	5.33E-3	1.9
	64	1.15E-5	3.4	1.07E-3	2.1	1.35E-3	2.0	1.35E-3	2.0
	128	7.98E-7	3.8	2.28E-4	2.2	3.36E-4	2.0	3.39E-4	2.0

Table 5: Error and Order of Convergence in the Derivative of the Solution of Example 2 Measured on $\Delta_0 = \{1/8, 1/4, 3/8, \ldots, 7/8\}$.

METHOD	N	$\varepsilon = 10^{-2}$		10^{-4}		10^{-6}		10^{-8}	
		$\|\|e\|\|_{h,\Delta}$	r	$\|\|e\|\|_{h,\Delta}$	r	$\|\|e\|\|_{h,\Delta}$	r	$\|\|e\|\|_{h,\Delta}$	r
1	4	7.35E-3		1.54E-4		1.57E-6		1.57E-8	
	8	3.83E-3	0.9	8.75E-5	0.8	9.19E-7	0.8	9.21E-9	0.8
	16	3.99E-4	3.3	4.61E-5	0.9	4.76E-7	0.9	4.78E-9	0.9
	32	4.74E-5	3.1	1.35E-3	-4.9	2.38E-7	1.0	2.41E-9	1.0
	64	1.63E-5	1.5	2.81E-3	-1.1	8.28E-8	1.5	1.21E-9	1.0
	128	1.42E-6	3.5	6.32E-4	2.2	9.01E-7	-3.4	6.01E-10	1.0
3	4	3.13E-2		4.66E-4		4.67E-6		4.67E-8	
	8	2.93E-2	0.1	5.92E-4	-0.3	5.95E-6	-0.3	5.96E-8	-0.4
	16	2.21E-2	0.4	9.59E-4	-0.7	9.70E-6	-0.7	9.70E-8	-0.7
	32	7.52E-3	1.6	1.72E-3	-0.8	1.76E-5	-0.9	1.76E-7	-0.9
	64	9.96E-4	2.9	3.20E-3	-0.9	3.35E-5	-0.9	3.35E-7	-0.9
	128	6.75E-5	3.9	5.98E-3	-0.9	6.55E-5	-1.0	6.55E-7	-1.0
3T	4	4.93E-3		8.55E-5		8.65E-7		8.65E-9	
	8	1.05E-3	2.2	4.85E-5	0.8	5.06E-7	0.8	5.06E-9	0.8
	16	1.43E-4	2.9	2.86E-5	0.8	2.63E-7	0.9	2.63E-9	0.9
	32	6.88E-6	4.4	1.28E-3	-5.5	1.32E-7	1.0	1.32E-9	1.0
	64	2.15E-5	-1.6	8.97E-4	0.5	9.07E-8	0.5	6.65E-10	1.0
	128	2.00E-6	3.4	3.48E-4	1.4	8.80E-7	-3.3	3.35E-10	1.0

Table 6: Error and Order of Convergence for Example 2 Measured on $\Delta = \{0, h, 2h, \ldots, Nh = 1\}$.

METHOD	N	$\varepsilon = 10^{-2}$		10^{-4}		10^{-8}	
		$\|\|e\|\|_{h,\Delta_0}$	r_0	$\|\|e\|\|_{h,\Delta_0}$	r_0	$\|\|e\|\|_{h,\Delta_0}$	r_0
1	4	5.26E-1		5.70E-1		5.71E-1	
	8	2.57E-1	1.0	3.40E-1	0.7	3.41E-1	0.7
	16	9.60E-2	1.4	1.83E-1	0.9	1.83E-1	0.9
	32	1.79E-2	2.4	9.40E-2	1.0	9.50E-2	0.9
	64	1.88E-4	6.6	4.73E-2	1.0	4.83E-2	1.0
	128	1.20E-5	4.0	2.33E-2	1.0	2.43E-2	1.0
2	4	3.16E-1		6.06E-1		6.30E-1	
	8	1.00E-1	1.7	4.24E-1	0.5	4.53E-1	0.5
	16	1.45E-2	2.8	3.58E-2	3.6	3.43E-2	3.7
	32	1.97E-3	2.9	9.78E-3	1.9	1.02E-2	1.7
	64	1.76E-4	3.5	2.51E-3	2.0	2.66E-3	1.9
	128	1.25E-5	3.8	6.09E-4	2.0	6.76E-4	2.0
3	4	5.34E-2		2.84E-2		2.77E-2	
	8	2.12E-2	1.3	6.52E-3	2.1	6.26E-3	2.1
	16	2.45E-3	3.1	8.09E-4	3.0	8.10E-4	3.0
	32	1.45E-4	4.1	1.03E-4	3.0	1.03E-4	3.0
	64	8.46E-6	4.1	1.29E-5	3.0	1.30E-5	3.0
	128	5.00E-7	4.1	1.61E-6	3.0	1.63E-6	3.0
1P	4	2.74E-2		5.70E-1		5.71E-1	
	8	1.49E-2	0.9	1.51E-1	1.9	1.52E-1	1.9
	16	7.80E-4	4.3	8.41E-6	17.5	9.44E-6	14.0
	32	6.76E-5	3.5	2.09E-7	5.3	5.88E-7	4.0
	64	4.34E-6	4.0	3.29E-7	-0.7	3.67E-8	4.0
	128	2.72E-7	4.0	2.56E-8	3.7	2.29E-9	4.0

Table 7: Error and Order of Convergence for Example 3 Measured on $\Delta_0 = \{-3/4, -1/2, -1/4, 1/4, 1/2, 3/4\}$.

METHOD	N	$\varepsilon = 10^{-2}$		10^{-4}		10^{-8}	
		$\|\|e'\|\|_{h,\Delta_0}$	r_1	$\|\|e'\|\|_{h,\Delta_0}$	r_1	$\|\|e'\|\|_{h,\Delta_0}$	r_1
1	4	1.42E 0		1.71E 0		1.71E 0	
	8	1.36E 0	0.1	2.07E 0	-0.3	2.07E 0	-0.3
	16	3.10E-2	5.5	2.38E-4	13.1	5.07E-7	22.0
	32	2.78E-2	0.2	4.73E-4	-1.0	1.25E-7	2.0
	64	2.00E-2	0.5	6.71E-4	-0.5	6.00E-8	1.1
	128	1.39E-3	3.8	7.68E-4	-0.2	5.23E-8	0.2
2	4	1.90E 1		2.79E 3		2.91E 7	
	8	7.18E 0	1.4	1.18E 3	1.2	1.19E 7	1.3
	16	1.48E 0	2.3	3.45E 2	1.8	3.51E 6	1.8
	32	1.97E-1	2.9	9.03E 1	1.9	9.26E 5	1.9
	64	1.76E-2	3.5	2.26E 1	2.0	2.37E 5	2.0
	128	1.26E-3	3.8	5.49E 1	2.0	5.97E 4	2.0
3	4	8.01E-2		5.45E-4		5.39E-8	
	8	2.31E-1	-1.5	6.04E-4	-0.1	3.69E-8	0.5
	16	9.31E-3	4.6	3.75E-6	7.3	0.0	
	32	8.58E-4	3.4	8.72E-8	5.4	0.0	
	64	6.02E-5	3.8	4.88E-8	0.8	0.0	
	128	3.96E-6	3.9	2.45E-8	1.0	0.0	
1P	4	2.31E 0		1.71E 0		1.71E 0	
	8	4.16E-1	2.5	2.07E 0	-0.3	2.07E 0	-0.3
	16	4.43E-3	6.6	9.57E-3	7.8	9.55E-3	7.8
	32	1.87E-3	1.2	2.00E-3	2.3	2.08E-3	2.2
	64	1.12E-4	4.1	8.03E-4	1.3	6.77E-4	1.6
	128	7.52E-6	3.9	9.36E-5	3.1	1.90E-4	1.8

Table 8: Error and the Order of Convergence in the Derivative of the Solution of Example 3 Measured on $\Delta_0 = \{-3/4, -1/2, -1/4, 1/4, 1/2, 3/4\}$.

ETHOD	N	$\varepsilon = 10^{-2}$		10^{-4}		10^{-6}		10^{-8}	
		$\|\|e\|\|_{h,\Delta}$	r	$\|\|e\|\|_{h,\Delta}$	r	$\|\|e\|\|_{h,\Delta}$	r	$\|\|e\|\|_{h,\Delta}$	r
1	4	5.26E-1		5.70E-1		5.70E-1		5.71E-1	
	8	2.57E-1	1.0	3.40E-1	0.7	3.41E-1	0.7	3.41E-1	0.7
	16	9.60E-2	1.4	1.83E-1	0.9	1.83E-1	0.9	1.83E-1	0.9
	32	1.81E-2	2.4	9.40E-2	1.0	9.50E-2	0.9	9.50E-2	0.9
	64	1.91E-4	6.6	4.73E-2	1.0	4.83E-2	1.0	4.83E-2	1.0
	128	1.22E-5	4.0	2.33E-2	1.0	2.43E-2	1.0	2.43E-2	1.0
2	4	3.16E-1		6.06E-1		6.25E-1		6.30E-1	
	8	1.00E-1	1.7	4.24E-1	0.5	4.51E-1	0.5	4.53E-1	0.5
	16	1.77E-2	2.5	2.99E-1	0.5	3.66E-1	0.3	3.68E-1	0.3
	32	2.11E-3	3.1	1.82E-1	0.7	3.38E-1	0.1	3.42E-1	0.1
	64	1.84E-4	3.5	6.09E-2	1.6	3.20E-1	0.1	3.35E-1	0.0
	128	1.31E-5	3.8	9.39E-3	2.7	2.88E-1	0.2	3.33E-1	0.0
3	4	5.34E-2		9.22E-2		9.29E-2		9.29E-2	
	8	2.12E-2	1.3	7.25E-3	3.7	7.48E-3	3.6	7.48E-3	3.6
	16	5.68E-3	1.9	1.52E-2	-1.1	8.10E-4	3.2	8.10E-4	3.2
	32	3.02E-4	4.2	4.19E-2	-1.5	6.90E-4	0.2	1.03E-4	3.0
	64	1.89E-5	4.0	1.89E-2	1.1	2.68E-3	-2.0	2.80E-5	1.9
	128	1.19E-6	4.0	1.49E-2	0.3	1.00E-2	-1.9	1.09E-4	-2.0
1P	4	2.74E-2		5.70E-1		5.71E-1		5.71E-1	
	8	1.49E-2	0.9	4.37E-1	0.4	4.45E-1	0.4	4.45E-1	0.4
	16	3.27E-3	2.3	1.34E-1	1.7	1.43E-1	1.6	1.43E-1	1.6
	32	1.93E-4	4.1	2.94E-2	2.2	3.77E-2	1.9	3.78E-2	1.9
	64	1.33E-5	3.9	2.89E-2	0.0	9.50E-3	2.0	9.59E-3	2.0
	128	8.28E-7	4.0	8.06E-3	1.8	2.32E-3	2.0	2.41E-3	2.0

Table 9: Error and Order of Convergence for Example 3 Measured on $\Delta = \{-1, -1+h, -1+2h, \ldots, -1+Nh = 1\}$.

Figure Captions

Figure 1: Canonical basis functions $\eta_0(s,\rho)$ and $\eta_1(s,\rho)$ on $-1 \leq s \leq 1$ for $\rho = 0.01$ (Figure 1a) and $\rho = 10$ (Figure 1b).

Figure 2: Solution of Example 1 using cubic polynomials and collocation at the Gauss-Legendre points.

Figure 3: Error $||e(h)||_{\Delta_0}$ for Example 1 using Methods 1, 2, and 3 and measured on the partition $\Delta_0 = \{1/8, 1/4, 3/8, \ldots, 7/8\}$.

Figure 4: Solutions of Example 1 using Methods 1, 2, and 3 on $0 \leq x \leq 1/4$ for $\varepsilon = 10^{-4}$ and $h = 1/8$.

Figure 5: Error $e(x)$ and its derivative $e'(x)$ in the solution of Example 1 by Method 1 for $\varepsilon = 10^{-4}$ and $h = 1/8$. (Note: $e'(0) = -5.76 \times 10^3$.)

Figure 6: Error $e(x)$ and its derivative $e'(x)$ in the solution of Example 1 by Method 2 for $\varepsilon = 10^{-4}$ and $h = 1/8$.

Figure 7: Error $e(x)$ and its derivative $e'(x)$ in the solution of Example 1 by Method 3 for $\varepsilon = 10^{-4}$ and $h = 1/8$. (Note: $e'(0) = 1.0 \times 10^4$.)

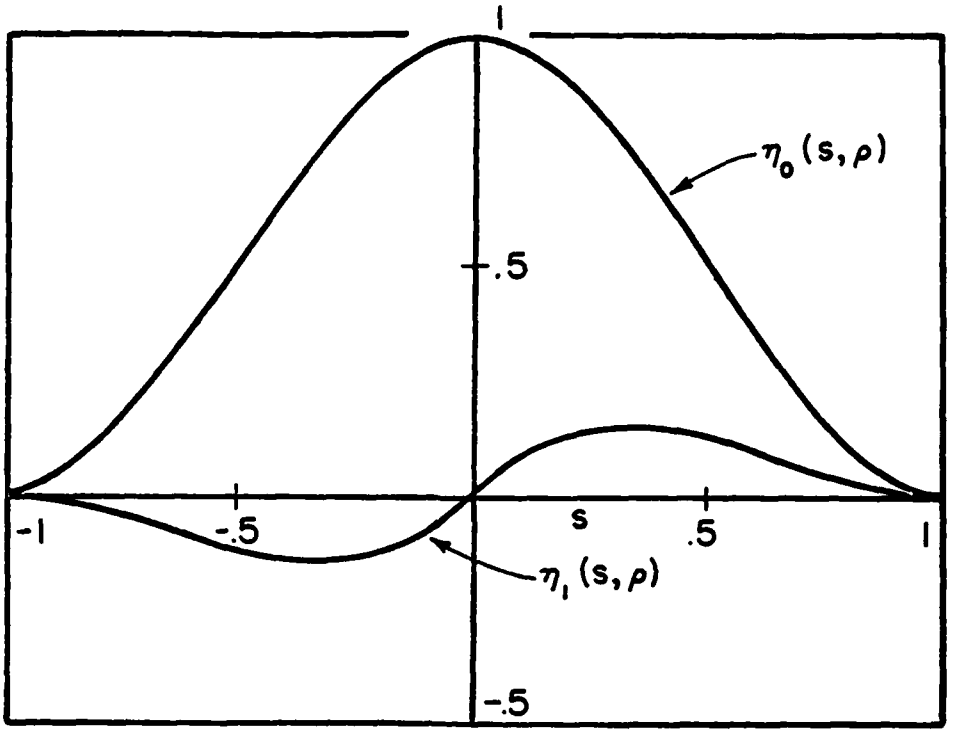
1
$\eta_0(s,\rho)$
.5
-1
-.5
s
.5
1
$\eta_1(s,\rho)$
-.5

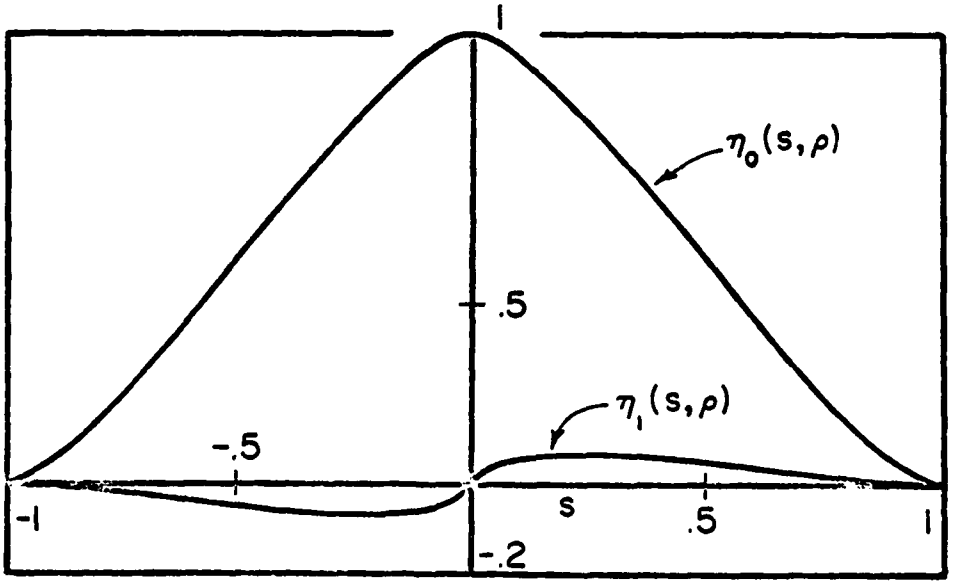
1
$\eta_0(s,\rho)$
.5
$\eta_1(s,\rho)$
-.5
-1
s
.5
1
-.2

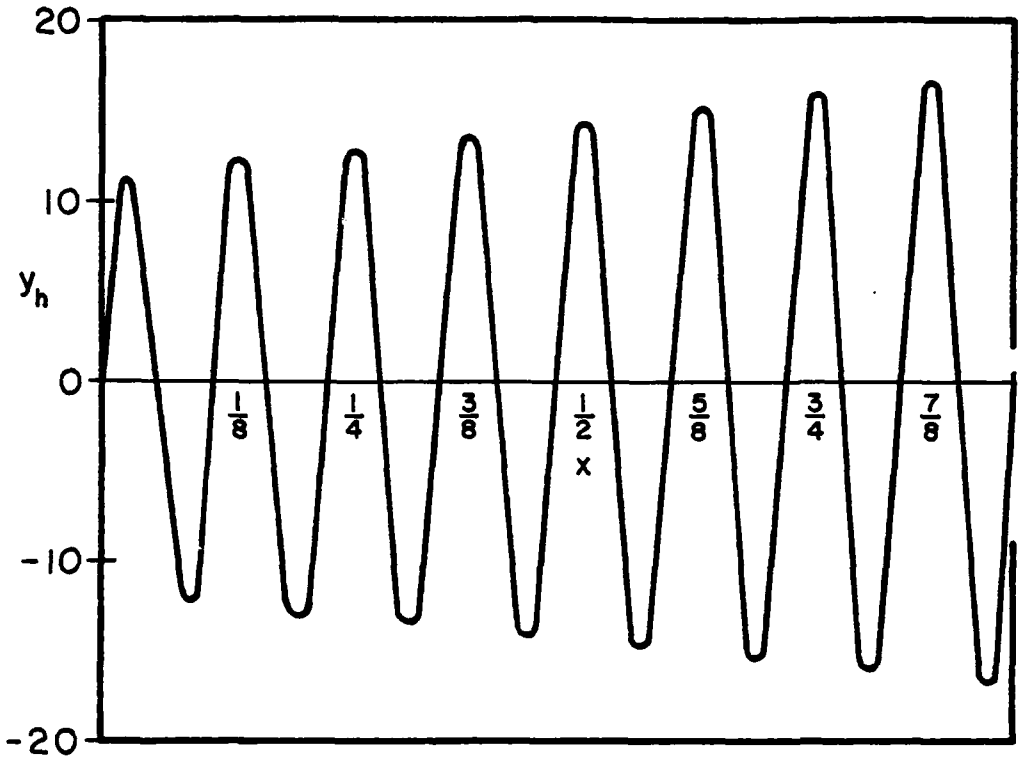
20
10
0
-10
-20
y_h
$\frac{1}{8}$
$\frac{1}{4}$
$\frac{3}{8}$
$\frac{1}{2}$
$\frac{5}{8}$
$\frac{3}{4}$
$\frac{7}{8}$
x

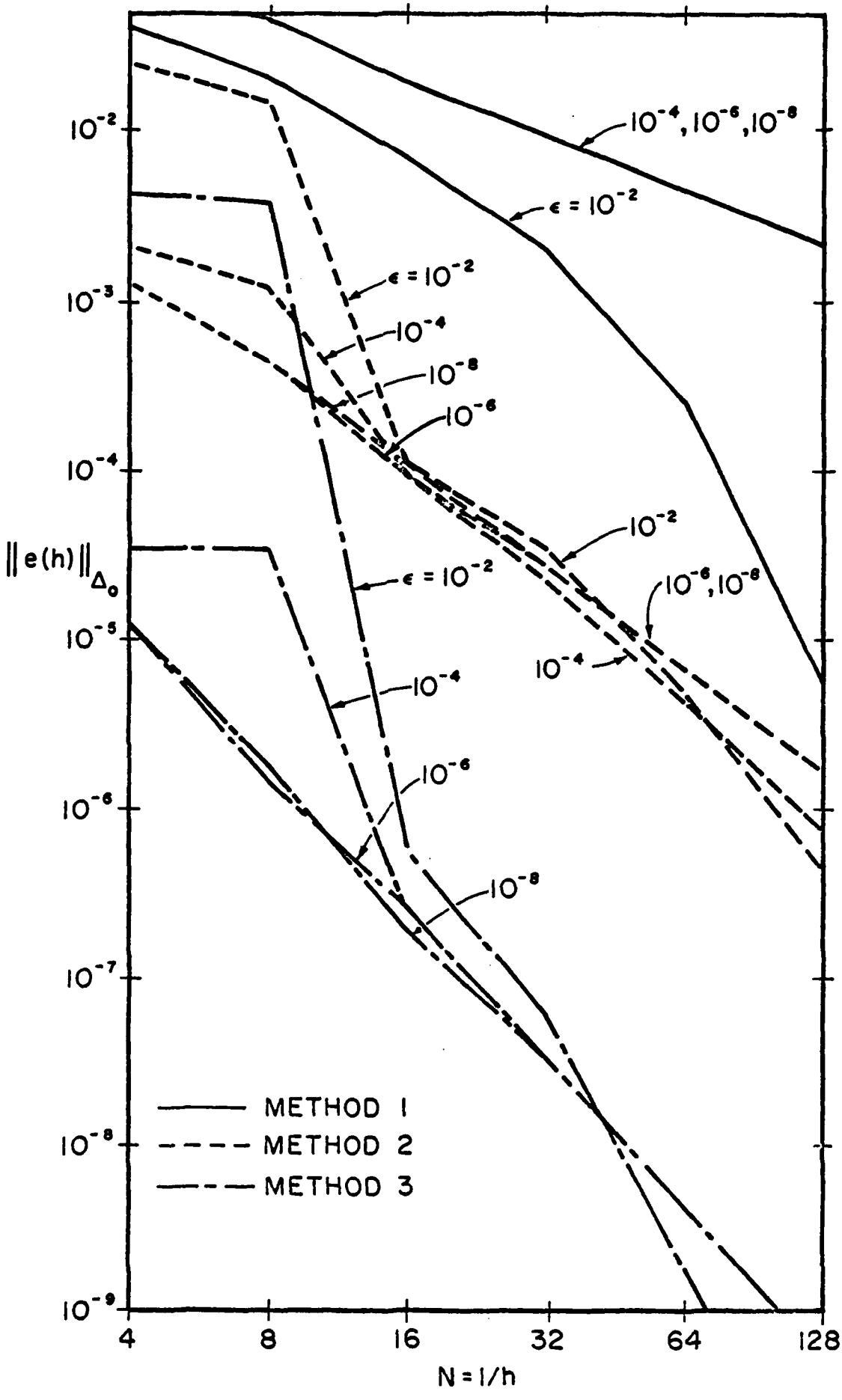
10^{-2}
10^{-3}
10^{-4}
10^{-5}
10^{-6}
10^{-7}
10^{-8}
10^{-9}
$\|e(h)\|_{\Delta_0}$
4
8
16
32
64
128
N = 1/h
$10^{-4}, 10^{-6}, 10^{-8}$
$\epsilon = 10^{-2}$
$\epsilon = 10^{-2}$
10^{-4}
10^{-8}
10^{-6}
10^{-2}
$\epsilon = 10^{-2}$
$10^{-6}, 10^{-8}$
10^{-4}
10^{-4}
10^{-6}
10^{-8}
METHOD 1
METHOD 2
METHOD 3

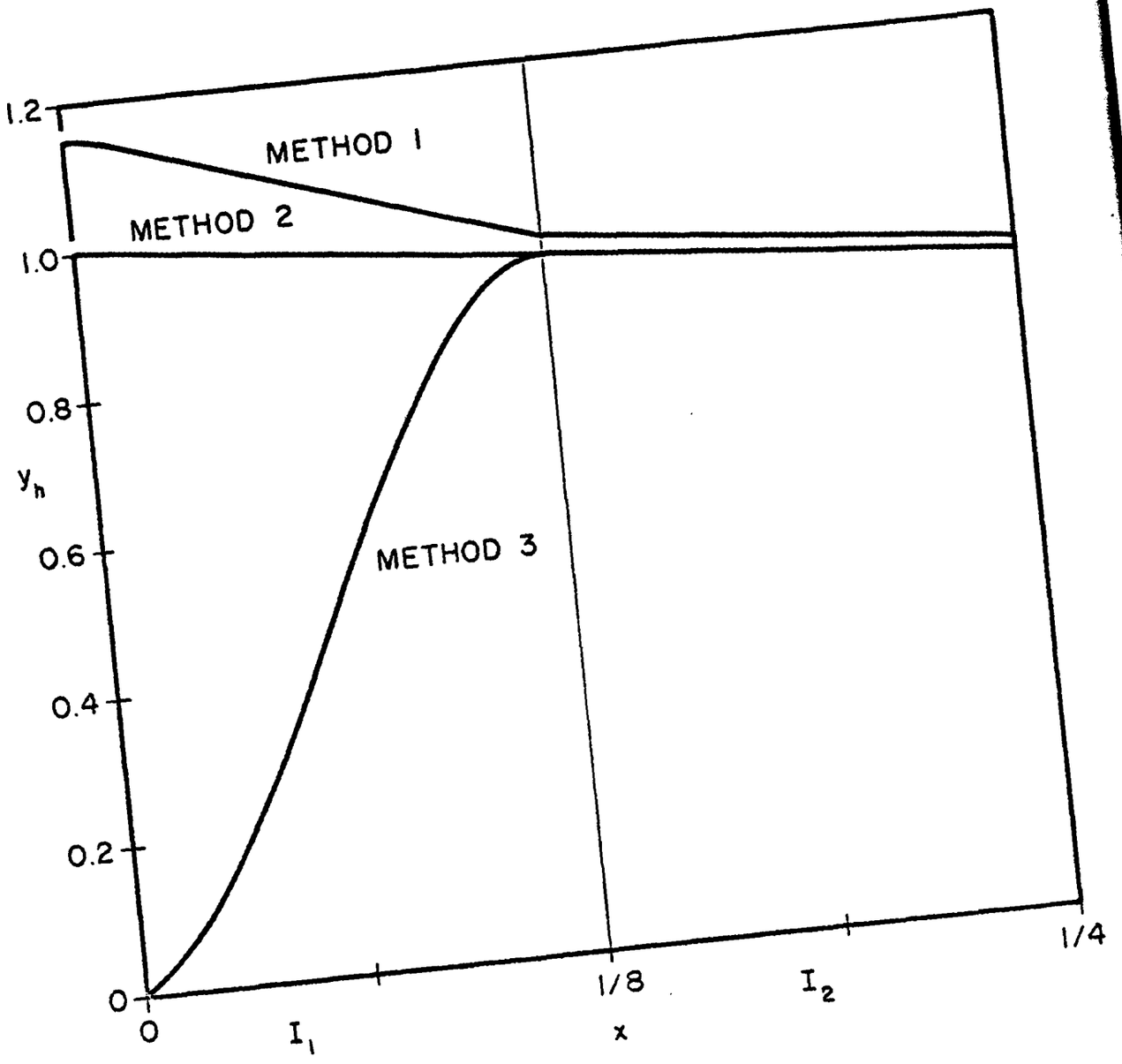
1.2
METHOD 1
METHOD 2
1.0
0.8
y_h
0.6
METHOD 3
0.4
0.2
0
0
I_1
1/8
x
I_2
1/4

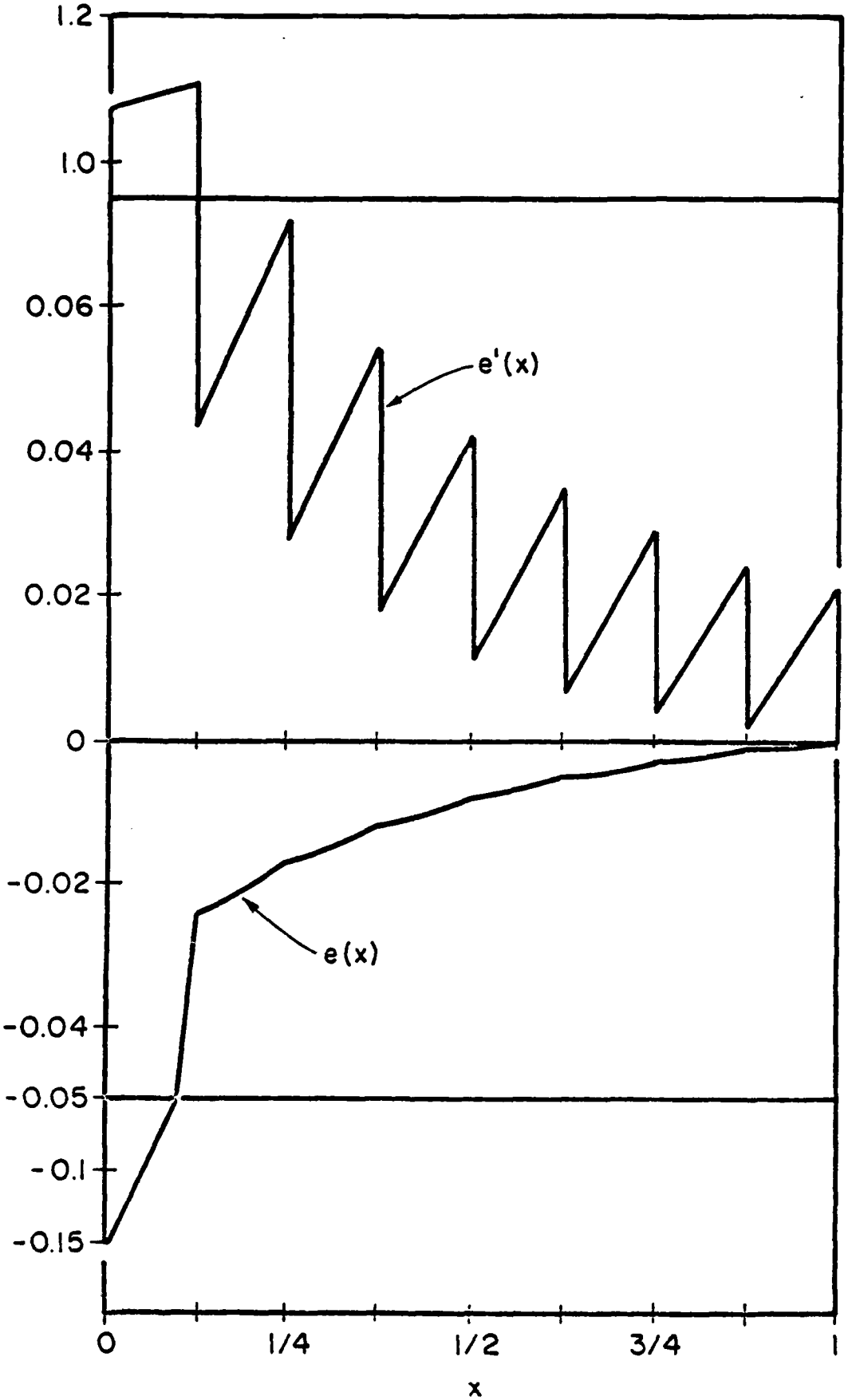
1.2
1.0
0.06
0.04
0.02
0
-0.02
-0.04
-0.05
-0.1
-0.15
e'(x)
e(x)
0
1/4
1/2
3/4
1
x

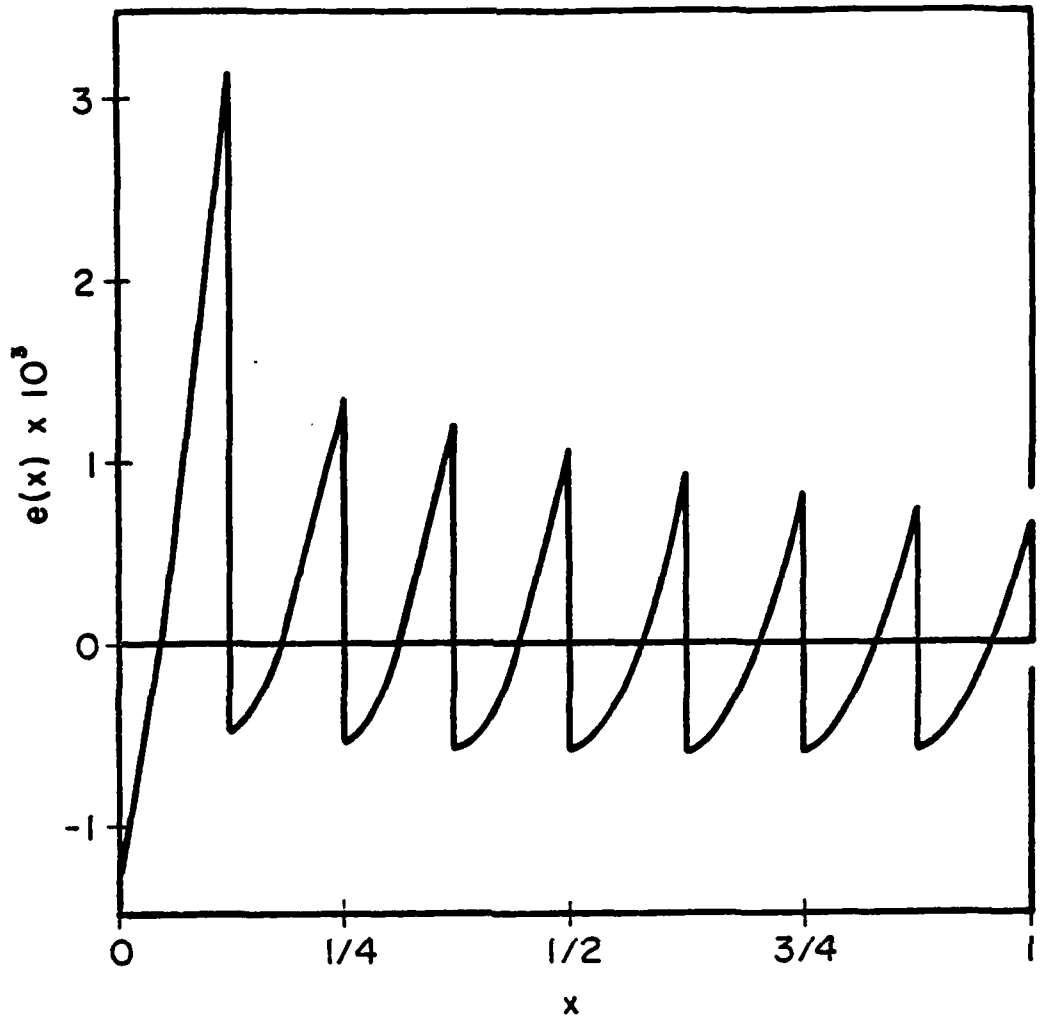
3
2
1
0
-1
e(x) x 10³
0
1/4
1/2
3/4
1
x

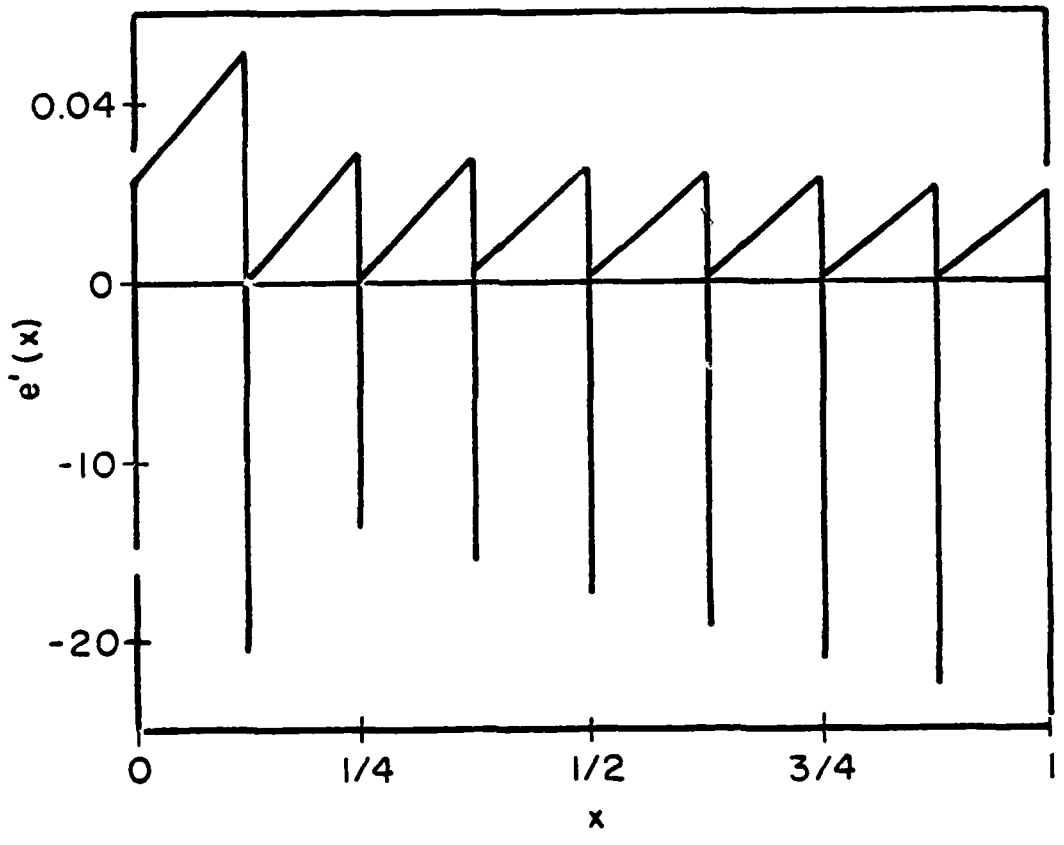
0.04
0
-10
-20
e'(x)
0
1/4
1/2
3/4
1
x

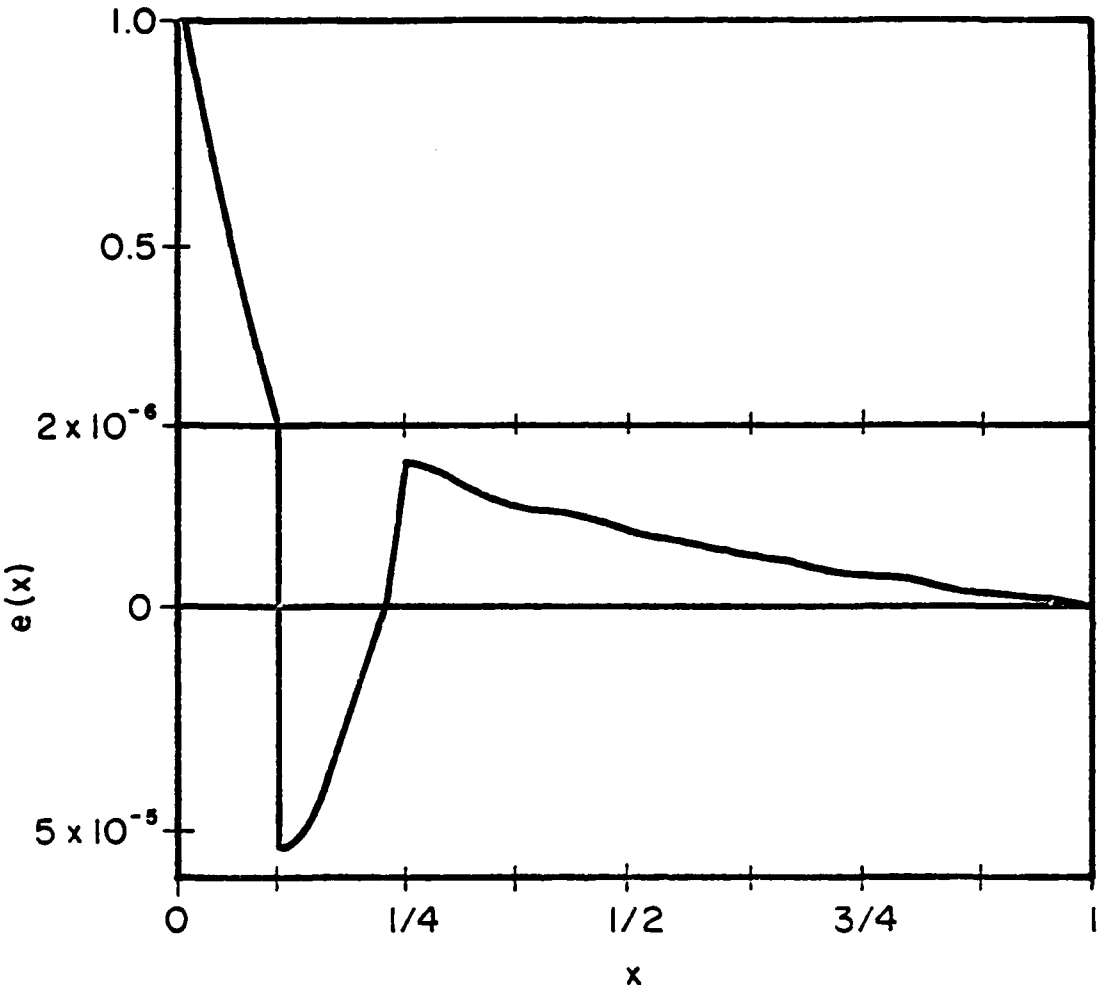
1.0
0.5
2 x 10^-6
0
5 x 10^-5
e(x)
0
1/4
1/2
3/4
1
x

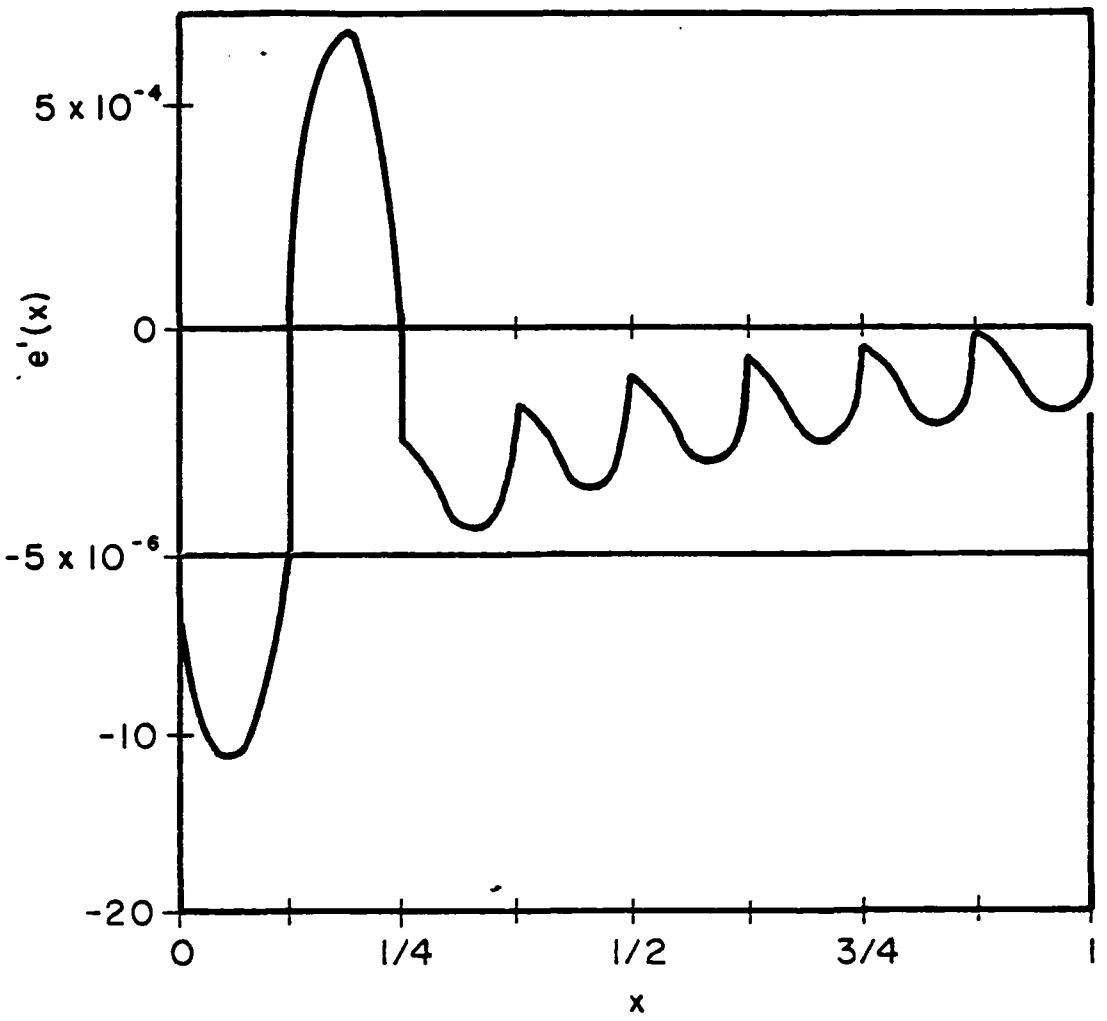
5 x 10^-4
0
-5 x 10^-6
-10
-20
e'(x)
0
1/4
1/2
3/4
1
x

UNCLASSIFIED

SECURITY CLASSIFICATION OF THIS PAGE *(When Data Entered)*

REPORT DOCUMENTATION PAGE	READ INSTRUCTIONS BEFORE COMPLETING FORM
1. REPORT NUMBER **AFOSR-TR- 80-0085** 2. GOVT ACCESSION NO.	3. RECIPIENT'S CATALOG NUMBER
4. TITLE *(and Subtitle)* COLLOCATION WITH POLYNOMIAL AND TAUT SPLINES FOR SINGULARLY PERTURBED BOUNDARY VALUE PROBLEMS	5. TYPE OF REPORT & PERIOD COVERED Interim
	6. PERFORMING ORG. REPORT NUMBER
7. AUTHOR(s) Joseph E. Flaherty and William Mathon	8. CONTRACT OR GRANT NUMBER(s) AFOSR 75-2818
9. PERFORMING ORGANIZATION NAME AND ADDRESS Rensselaer Polytechnic Institute Department of Mathematical Sciences Troy, New York 12181	10. PROGRAM ELEMENT, PROJECT, TASK AREA & WORK UNIT NUMBERS 61102F 2304/A3
11. CONTROLLING OFFICE NAME AND ADDRESS Air Force Office of Scientific Research/NM Bolling AFB, Washington, DC 20332	12. REPORT DATE November, 1979
	13. NUMBER OF PAGES 49
14. MONITORING AGENCY NAME & ADDRESS*(if different from Controlling Office)*	15. SECURITY CLASS. *(of this report)* UNCLASSIFIED
	15a. DECLASSIFICATION/DOWNGRADING SCHEDULE

16. DISTRIBUTION STATEMENT *(of this Report)*

Approved for public release; distribution unlimited

17. DISTRIBUTION STATEMENT *(of the abstract entered in Block 20, if different from Report)*

18. SUPPLEMENTARY NOTES

Submitted to - SIAM J. SCI. & STAT. COMP.

19. KEY WORDS *(Continue on reverse side if necessary and identify by block number)*

Singular Perturbations, stiff differential equations, collocation, asymptotics, boundary value problems, taut splines

20. ABSTRACT *(Continue on reverse side if necessary and identify by block number)*

Collocation methods using both cubic polynomials and splines in tension are developed for second order linear singularly-perturbed two-point boundary value problems. Rules are developed for selecting tension parameters and collocation points. The methods converge outside of boundary layer regions without the necessity of using a fine discretization. Numerical examples comparing the methods are presented.

DD FORM 1 JAN 73 1473

UNCLASSIFIED